# Jupiter in 2000/2001

## Part II: Infrared and ultraviolet wavelengths – A review of multispectral imaging of the jovian atmosphere

**John H. Rogers, Tomio Akutsu & Glenn S. Orton**

*A report of the Jupiter Section (Director: John H. Rogers)*

In 2000/2001, Jupiter was imaged at more wavelengths more intensively than ever before. This paper reviews the data sets available, and reports on the major features detected in them, especially a novel pattern of large scale waves over the North Equatorial Belt (NEB). The images came from amateur contributors, from the NASA Infrared Telescope Facility, and from the *Cassini* and *Galileo* spacecraft. Images were taken not only in visible wavelengths, but also in the ultraviolet and in the near-infrared methane absorption bands (all these wavelengths being sensitive to levels above the main cloud layers); in near-infrared continuum bands (penetrating within the main cloud layers); and in the mid-infrared thermal band (revealing emission from below the cloud layers).

Polar hoods and anticyclonic ovals were, as usual, among the most prominent bright features in the methane-band images. These images also revealed major disturbances affecting the South and North Equatorial regions. The South Equatorial Disturbance, a solitary wave in the visible clouds, showed massive disruption of the upper haze layers in the infrared (see Paper III of this report).

The NEB waves were a series of large diffuse methane-dark patches, representing variations in the thickness of high-altitude haze over the belt, with a 'wavelength' of 20–25° longitude. The most conspicuous of the patches were aligned with visible features, particularly the preceding sides of visible barges, where there was anticyclonic eddying. Longitude measurements show that the waves moved at the same speeds as the underlying visible features, i.e. in the range between System II and System III, and anomalies in their motion were related to visible cloud events. There was no sign of any phase speed that was different from the speed of the underlying visible features. Therefore the waves were controlled by the lower-lying tropospheric circulations.

These NEB waves in 2000/2001 may have been a consequence of the ongoing NEB broadening event, and they became indistinct just as the NEB broadening became complete. They had many similarities to 'slow-moving thermal waves' reported by previous mid-infrared observers, which were also most conspicuous when barges were present. We propose that these waves are induced by the curving and eddying of the tropospheric NEBn jetstream, and that they propagate upwards as warm waves which cause thinning of the high-altitude haze as well as enhanced mid-infrared emission.

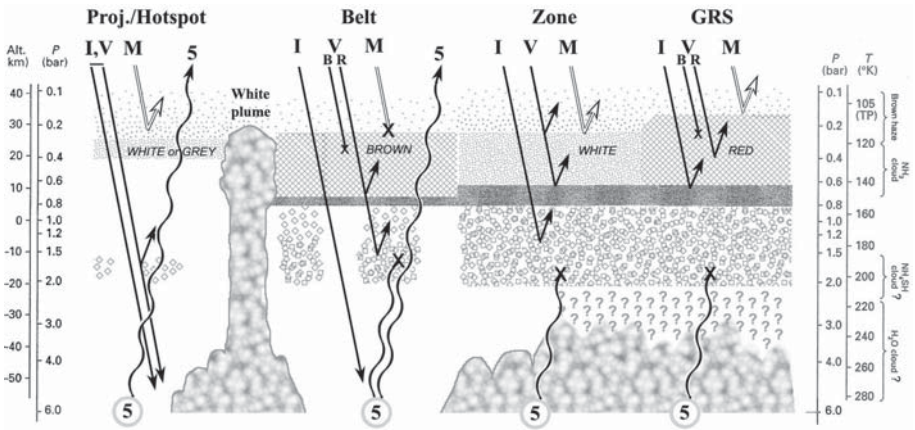


**Figure 1.** Diagram of Jupiter's atmosphere, summarising the probable levels of the various cloud layers. Scales give the altitude (km), pressure (one bar is the atmospheric pressure at Earth's surface) and temperature (Kelvin). The diagram shows typical ray-paths for visible (V) including blue (B) and red (R), I-band (I), methane (M), and 4.8μm (5) radiation; x indicates absorption of the rays. This is adapted from Figure 4.28 of ref.5, taking account of more recent analyses including ref.6. The diagram shows thick cloud layers around 0.8 bars, and patchy layers with larger particles between 1 and 2 bars. As discussed in the text, these layers could be the same; however, such disagreements between different studies may not be of fundamental importance. Even in Earth's atmosphere, with only one condensible vapour, there are often several layers of clouds with different properties and drifts; so in Jupiter's atmosphere, with several condensible vapours, similar complexity would not be surprising.

## Introduction

Jupiter has never been studied with higher resolution and frequency than it was in 2000/2001, not only in the visible waveband,[1] but also in other wavebands from the infrared to the ultraviolet. Multispectral imaging was carried out by amateur observers, by spacecraft, and by professional observatories. This great effort was partly due to the unprecedented dual flyby by the *Cassini* and *Galileo* spacecraft,[2] and partly due to the recent improvements in both amateur and professional ground-based detectors. These multispectral observations provide three-dimensional views of Jupiter's clouds, giving new insight into the dynamics of the atmosphere.

In a previous report,[3] we reviewed the imaging of Jupiter in the near-infrared methane absorption band at 890nm, which is now being carried out by several amateur observers as well as by spacecraft. In this report, we consider the imaging in all near-infrared (IR) and ultraviolet (UV) wavebands during 2000/2001, reviewing the data sets available, and describing the major features detected in them. Feature numbers are taken from our report on observations in visible light (reference 1, hereafter Paper I). As the planet was in a largely typical state, this will serve as a review of multispectral probing of the jovian atmosphere.

Table 1 summarises the wavebands which have been accessed by different observatories. Figure 1 shows how they penetrate to different levels in the atmosphere, relative to the various cloud layers presently believed to exist.

UV and visible and methane-band light are affected mainly by three well-established layers of haze or cloud.[4–6] The topmost is a very thin haze in the stratosphere, probably made of molecules produced by the actions of sunlight or aurorae. (Ultraviolet and methane-band images are sensitive to this haze and to the upper extent of the denser haze below.) The next layer is a denser but still diffuse haze, filling the whole of the upper troposphere down to the main visible clouds. It is brown ('violet-absorbing' or 'reddish') and may be a mixture of the brown aerosols settling from above and the white ammonia-ice cirrus from below. The density seems to be fairly constant but the degree of (ultra-)violet absorption is variable and accounts for the main colour differences on the planet; it gives the brown colour to belts and the red colour to the GRS. Thirdly comes the main visible cloud-top, at ~0.5 to 0.7 bars, which is white, and almost certainly made of ammonia ice. This layer is opaque to all wavelengths in the bright zones, but partly transparent or even absent in the dark belts and dark streaks.

UV wavelengths sense high levels in the atmosphere. Mid-UV, as detected by *Cassini* (and by the Hubble Space Telescope [HST]), is scattered by gas above the visible clouds, but also absorbed by the ubiquitous 'brown haze' at the same levels. This gives the brown colour to belts and to reddish anticyclonic ovals, which therefore appear dark in UV. Near-UV, as imaged by amateurs, penetrates the gas but is absorbed by the brown haze slightly deeper than mid-UV.

Violet and deep blue light are absorbed by the same diffuse brown haze. This is why they show strong contrast between belts and zones but little detail within them. Longer visible wavelengths are progressively less subject to this absorption and penetrate increasingly deep into the main cloud layers, where most of the meteorology and most of the visible structure is found. In zones, the main cloud layer is opaque at all wavelengths, so we do not know how deep it extends. But in belts, red and near-infrared (I-band) light does penetrate the ammonia cloud level; dark brown belt regions display a combination of the brown haze ranging from high levels down to a thin cloud layer at ~0.9 bar, and a fairly clear and therefore dark atmosphere below.[6,7] In dark grey or bluish-grey streaks (including the NEBs projections or 'hotspots'), the brown haze is not so thick and much light penetrates into clear deep air; what little light is scattered back is slightly bluish like the blue sky of Earth. (The absence of polarisation, which at one time was thought to rule out this model, is now attributable to the ubiquitous high-altitude haze layer.)

How deep the red and infrared wavelengths penetrate in the belts, and what cloud layers are found there, is still a subject of debate. Data from different approaches have often been difficult to reconcile, and in spite of years of analysis of data from advanced telescopes and even from spacecraft, we have to humbly admit that Jupiter is still a frustratingly distant and alien planet. Theoretical modelling from the observed chemical composition predicted cloud layers of ammonum hydrosulphide at 1.5 to 2 bars, and of water at 4-6 bars.[8] Mid-infrared spectra imply that the main visible and 5-micron-absorbing cloud layers indeed lie at 1.5 to 1.8 bars, according to the most recent analyses of data from *Voyager*[7] and from *Galileo*'s Near-Infrared Mapping Spectrometer (NIMS).[9–12] However, methane-band images are more consistent with the main visible cloud layers being at 0.65 to 0.95 bar,[6] with few clouds underneath down to >> 4 bar.

Finally, the *Galileo* Probe found almost no clouds on its descent path – but that is because it entered a NEBs projection/hotspot which is now known to be a uniquely clear dry weather system.[13–15] The main opacity in these weather systems is upper tropospheric haze (~0.3 bar), above the level at which the Probe started recording.[12,16]

The authors of the different *Galileo* studies agree that the differences are likely to be resolvable, partly due to the much higher resolution of the Solid State Imager (SSI) images, and partly due to the fact that the SSI and NIMS experiments are sensitive to clouds at different levels and particle sizes. SSI views the top of the clouds, while NIMS is sensitive to thermal emission from below them. In mixed cloud regions there is an ammonia condensate cloud layer at ~0.5–0.9 bars which is

**Table 1. Data sets in infrared and ultraviolet, 2000/2001**

| | | *Ultraviolet* | *Visible* | *Continuum* | *Near-infrared Weak methane* | *Strong methane* | *Mid-infrared (Thermal)* |
|---|---|---|---|---|---|---|---|
| *Amateur* | | | | | | | |
| T. Akutsu (Japan) | | 360 (broad) | R,G,B | 820 (broad) | | 893(*6.5 ) | |
| A. Cidadão (Portugal) | | 355 (*35) | R,G,B | 830(—>1000) | | 889(*5) | |
| B. Colville (Canada) | | 364 (*32) | R,G,B | 800 (*350) | | 889(*18) | |
| *Spacecraft* | | | | | | | |
| Cassini | ISS | 255 | R,G,B | 756 | 619, 727 | 891(*10) | |
| Galileo | SSI | | Violet | 756 | 727 | 889(*16) | |
| | NIMS | | | Range | Range | Range | Range |
| NASA-IRTF (Hawaii) | | | | 1.6μm | 3.8μm | 2.3μm | 4.8μm |

(Wavelengths in nm except for IRTF. (*) is full width at half-maximum (FWHM) of the filter, in nm.)

*Note: South is up in all images.*

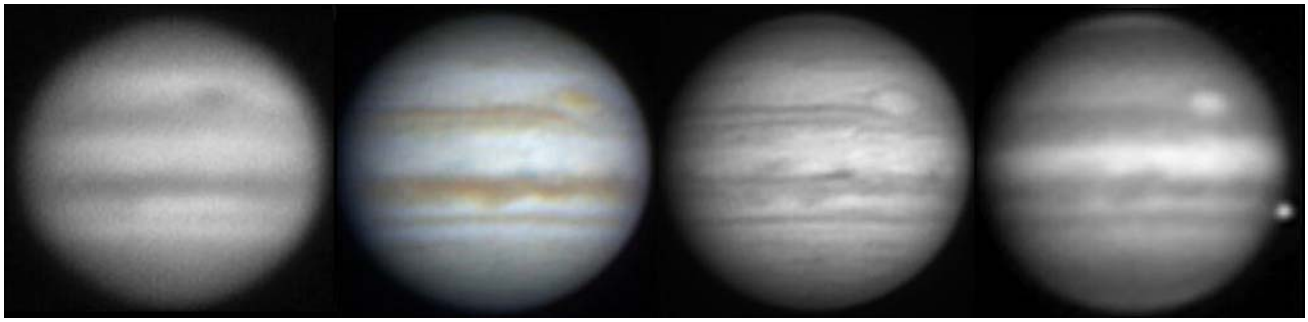

**Figure 2.** A typical set of images by Akutsu: UV (2000 Sep 14d 17h 16m UT, CM1=245, CM2=59); Visible RGB colour (Sep 19d 15h 52m UT, CM1=263, CM2=39); I-band (15h55m); $CH_4$ (15h58m). Shows GRS with SED passing it (main complex; in visible and I-band the rift is the only conspicuous element, and in methane there is a large discontinuity). Also shows NEBn bulge no.1b on CM (barge B1 is not resolved; spot no.1a has just appeared and is very dark in I-band), with NEB waves in methane band. Compare with Figure 3 and images from Sep 20–26 in Figure 5 of Paper I, showing the SED and NTropC spot 1a prograding relative to other features.

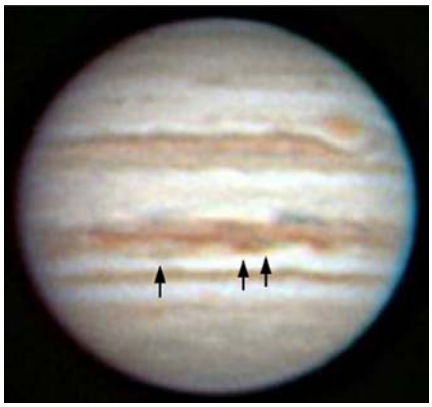

**Figure 3.** RGB colour image, 2000 Sep 30d 09h 45m, CM1=336.5, CM2=30.5, by David Moore. Arrows indicate the NTropC features no.1a (or a pre-existing spot), no.1b, and barge B1. Compare with Figure 2 and Figure 9.

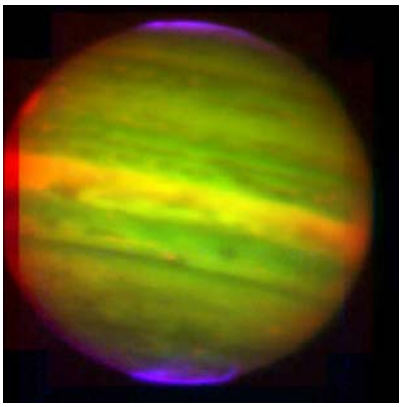

**Figure 5.** False-colour composite of IRTF images on Dec 18. Blue, 3.55μm; green, 1.6μm; red, 3.8μm. The GRS appears red on the p. limb; the SED main complex is near the f. limb. Green and yellow colours highlight clouds at various levels; purple emission is from the aurora. See Figure 14 for original images.

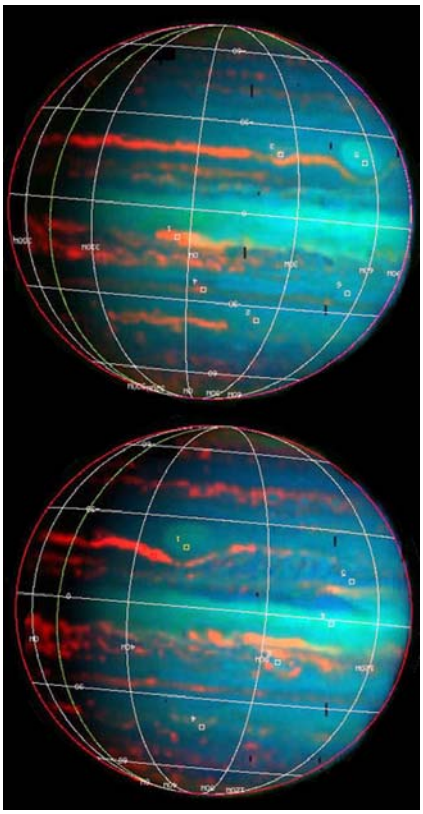

**Figure 6.** Two of six false-colour *Galileo* NIMS index images which covered the entire planet on 2000 Dec 31. Blue= weak methane, green= I-band, red= thermal. The disk is gibbous in reflected light but thermal emission (red) is seen equally on the night and day sides. In the second image, the GRS is on the CM and the SED main complex is near the f. limb. (Compare IRTF images on cover of ref.2.) Small squares indicate areas studied in more detail. *NASA*/Galileo *NIMS team.*

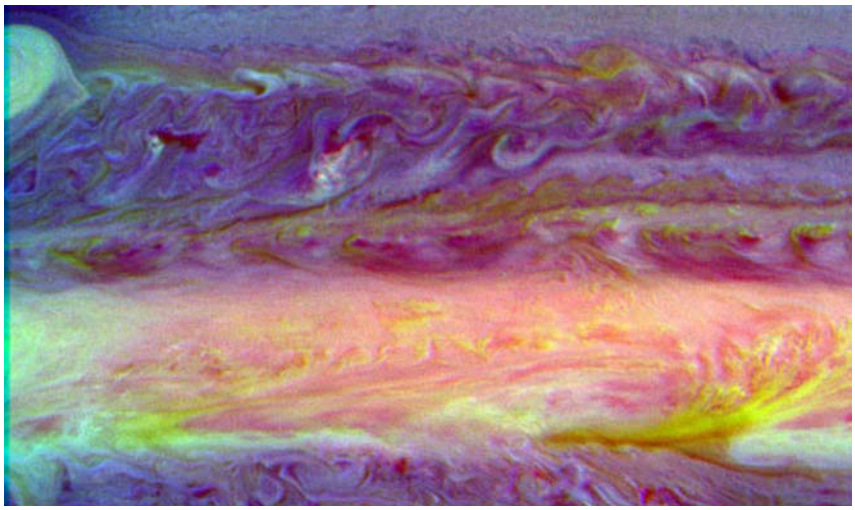

**Figure 4.** A false-colour composite from publicly released *Cassini* ratio images[26] displaying different degrees of methane absorption, encoding the different levels of the clouds. Blue= 619nm, weakest methane, deep levels; green= 727nm, weak methane, intermediate levels; red= 890nm, strong methane, high levels. The GRS, at top left, has clouds at all levels. The SEB f. it has little cloud except at deep levels, but small spots are bright at all levels indicating towering thunderclouds. The NEBs projection and festoon at lower right appears yellow, implying high and intermediate haze but no deep cloud. P. and f. it, the NEBs appears white implying clouds at all levels, suggesting that the darkness of this strip in visible light is due to dark cloud particles. The image set was taken on or close to 2000 Dec 15.

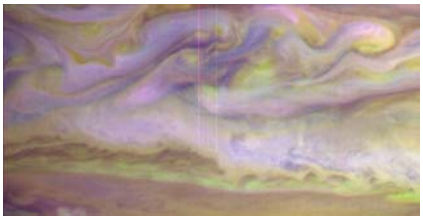

**Figure 7.** False-colour composite of *Galileo* images of the SEBZ, taken on 2001 Jan 1 at 04h UT. This is the p. end of the region shown in Figure 8, near the centre of Figure 4. Blue= violet; green= 756nm (I-band); red= 727nm (weak methane).

the main visible cloud in bright zones and which also might be the main cloud in darker belts. In belts, this layer is transparent to infrared radiation, perhaps because it consists of small particles to which the longer wavelengths are insensitive. Beneath this layer, there are more clouds at 1–2 bars which have larger particles that absorb longer IR wavelengths. Researchers for the *Galileo* SSI experiment[6] identify ~1.7-bar clouds in some especially dark holes in the NEB and SEB, and there could be more such cloud hidden beneath the thicker 0.9-bar cloud layer in surrounding regions. Others[9,10] suggest that light from the darker regions is predominantly reflected from clouds at 1–2 bars.

Even deeper, in NEBs projection/hotspots, all data agree that the air is generally clear with no water-cloud layer. However, both SSI and NIMS do detect patchy clouds at ~4 bars towards the edges of NEBs projection/hotspots.[6,11,17,18] This is probably water-cloud, and it is widely presumed to exist at the base of white plumes. Indeed, detailed *Galileo* study of white plumes in the mid-SEB f. the GRS has shown that they arise from a thick cloudtop at 4 bars with an opaque white plume-head rising to 0.4 bars, in which there is lightning – i.e. a giant thunderstorm;[19,20] recently confirmed by *Cassini*.[21] This makes it bright in weak methane bands and sometimes in strong methane bands.

Therefore, we can only give a tentative account of the layers sensed in different infrared wavebands (Figure 1). In the red and near-infrared continuum and pseudo-continuum, at various wavelengths from ~0.7 to 1.7μm, light penetrates into the ammonia cloud layer (in zones) or through it (in belts), revealing structure in the main cloud layers from ~0.7 bars to 2 bars. In some dark regions, as noted above, these wavelengths penetrate even deeper. Deeper levels can be viewed in the spectral 'window' around 5μm, where sunlight is dim, but bright thermal emission from deep in the planet is detected. This emission (from ~6–8 bars) is absorbed by the same cloud layers as the near-infrared continuum, i.e. the main cloud layers at 1–2 bars. Thus, while the zones are almost black at 5μm, the thinner clouds in the belts appear bright due to the emission from very deep levels. The 5μm transmission is closely correlated with visible colours.[22–24]

In addition, the near-infrared includes one hydrogen and several methane absorption bands.[3,19] Depending on the strength of the absorption, these wavelengths can penetrate to different depths into the atmosphere before being absorbed, and so they are selectively reflected from clouds lying above these levels. Weak methane bands at 619 and 727nm can be accessed with the narrow filters used on spacecraft, and reveal vertical structure in the main cloud layers as well as reflection from the overlying brown haze. The well-known band at 890nm is stronger and is mainly sensitive to the thickness of the overlying haze, which reflects this wavelength brightly. Around 2.3μm, the absorption by methane, molecular hydrogen, and even ammonia is even stronger, and the topmost haze layers are even more clearly revealed by their relatively bright reflectiveness. (These strong methane images are essentially a negative of the far-ultraviolet images, in which the high haze is dark because it absorbs the light.). At 3.5μm, the methane and ammonia absorption is so strong and the sunlight is sufficiently weak that the planet is essentially black, except for emission from aurorae.

# Data sets

### *Amateur observers*

The main multispectral imagers in 2000/2001 were Tomio Akutsu (Japan), Brian Colville (Canada), and Antonio Cidadão (Portugal; only in 2001 January). Their instruments and methane filters were listed in reference 3; their other filters are listed in Table 1. (This report also includes visible-light images by courtesy of other observers listed in Paper I.) A typical set of images from one of us (T. Akutsu) is shown in Figure 2. (All images in this paper have south up.)

The near-UV images show high contrast between the belts and zones, and the GRS is very dark. Otherwise only subdued details are visible, partly because the required long exposures make sharp images difficult, and partly because the high-level hazes that dominate these images are genuinely diffuse. However, they do occasionally record major changes: in 2001/2002 the UV images would record enhanced UV absorption in the EZ(N) as the most sensitive indicator of a long-awaited zonal coloration event.

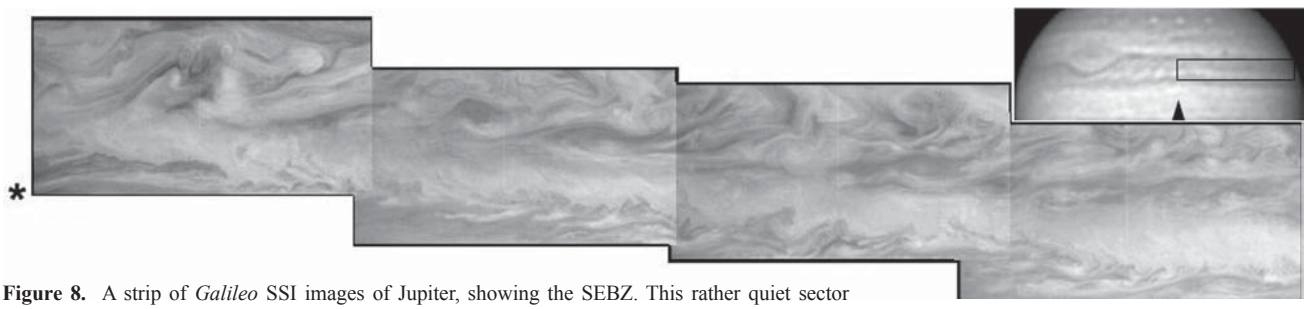


**Figure 8.** A strip of *Galileo* SSI images of Jupiter, showing the SEBZ. This rather quiet sector with small-scale turbulence is the only part to have been successfully imaged at the G29 encounter; it was just following the post-GRS turbulent sector and the SED. The SED main complex was just outside the Np. corner, as marked by an asterisk. The strip is made of 4 images centred from L2=124 (left) to 169 (right) (L3=103 to 148), taken on 2000 Dec 31 around 19h UT, at 756nm (I-band). South is approximately up. Images obtained from the NASA JPL Planetary Image Atlas[30]; images due to NASA and the Galileo SSI team, composited by JHR. (The strip was also imaged at 727nm. Also see Figure 7.)

*Inset right top*: The approximate area of the *Galileo* strip is boxed in this white-light image on 2001 Jan 1 at 23h14m UT, by A. Cidadão, CM1=44.5, CM2=105. The position of the SED main complex is arrowed; it was inconspicuous at the time. (The full colour image was on the cover of ref.2.)

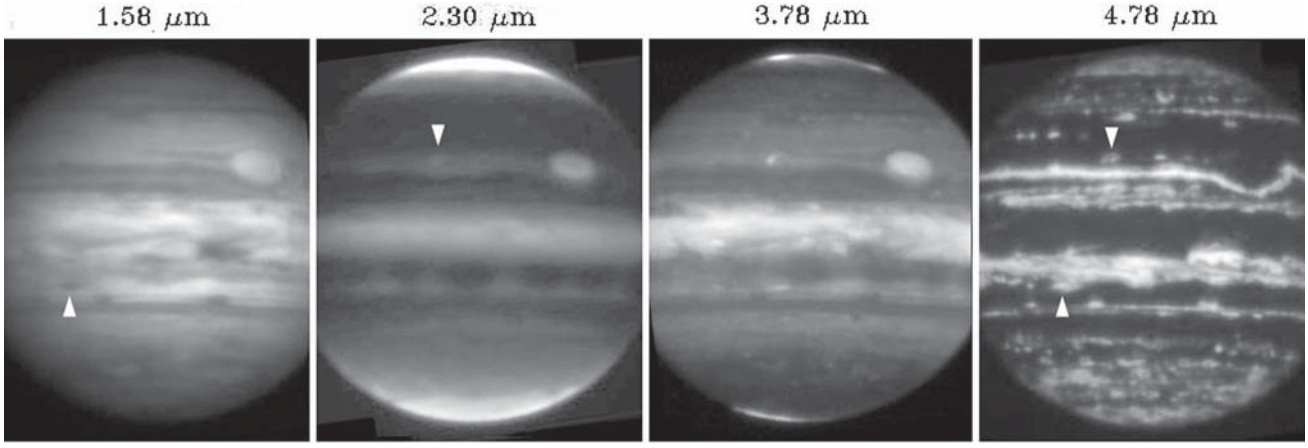


**Figure 9.** IRTF image set, 2000 Sep 29. This shows: (1) The GRS (at right); (2) STropC spot no.4 (brown oval in STropZ; arrowed; bright in methane and at 4.8μm); (3) The main complex of the SED (at extreme left); (4) On NEBn/NTropZ, NTropC spot no.1a and/or a pre-existing spot (arrowed), which is very dark at 1.6μm and bright at 4.8μm; and no.1b, a NEBn bulge on central meridian (barge B1 is not clearly seen at these wavelengths); (5) The series of NEB methane-dark waves, coinciding with NEBn bulges at 1.6 and 4.8μm, including the largest one in centre; (6) Two NTBs jetstream spots; (7) Fine detail in the NPR. Compare with near-IR images (Figure 2) and visible colour image (Figure 3).

The general features of I-band and methane images were described in our previous reports.[3,35] I-band images are useful for tracking spots (especially the bluish patches on the NEBs and SEBn which are very dark in I-band). Methane images, like UV images, show much less detail and less variability, but can record important phenomena which are less striking at visible wavelengths. In 2000/2001 the methane images recorded the spectacular phenomena of the NEB and SEB to be discussed below.

### *Cassini*

The NASA *Cassini* spacecraft began imaging Jupiter on 2000 October 1, and produced near-continuous imagery of the whole planet in multiple wavelengths from then until early December.[2,25,26] Closeups of selected regions were then taken in mid-December and for a few days around closest approach, which was on 2000 Dec 30. This was the first time since the *Voyager* mission that a spacecraft had continuously imaged the planet to follow its winds in all their wonderful detail, and *Cassini* had the advantage of a modern CCD imager, with filters ranging from UV to IR. A set of whole-disk images is in Figure 10. This article summarises features shown in the publicly-released images and movies, provided on websites.[25,26] All *Cassini* images are credited to NASA, JPL, the University of Arizona, and the *Cassini* imaging team led by Prof. Carolyn Porco. A preliminary report has very recently been published;[21] however, most of the data have yet to be released.

The appearance in the mid-UV waveband at 255nm (also used by the Hubble Space Telescope) was described in references 27–29. It routinely shows a negative of the methane image. This is because it is scattered very sensitively by gas but also absorbed very sensitively by the high-altitude brown haze; thus regions with thicker stratospheric haze appear darker.

The near-IR filters include continuum, weak methane, and strong methane, the latter being highly selective.[3] Examples are shown in ref.3, Figure 4 and Figure 10.

### *Galileo*

The *Galileo* Orbiter had only one perijove during the 2000/2001 apparition, the G29 encounter on 2000 Dec 28/29, coinciding with the *Cassini* flyby.[2] It was intended to target the turbulent SEBZ f. the GRS for coordinated observations, but unfortunately almost all of these images were lost due to radiation-induced faults in the SSI. The only region to have been successfully imaged is shown in Figures 7 and 8. However, *Galileo*'s Near-Infrared Mapping Spectrometer (NIMS) was fully functional and recorded images in selected IR wavelengths from 1.6 to 5.2μm; full-disk images covered the whole planet on Dec 31. Examples of the false-colour index images released are in Figure 6. (*Galileo* images are from the PDS website[30] and credited to NASA, JPL,and the *Galileo* teams.)

### *NASA Infrared Telescope Facility*

The NASA-IRTF is a 3.0m telescope on Mauna Kea, Hawaii. One of us (GSO) and colleagues obtained numerous images of Jupiter in near-infrared wavebands, using the near-infrared facility camera, NSFCAM. The images were taken during the NASA-IRTF Monitoring Program. This programme has taken place throughout the *Galileo* mission, with observations coordinated by GSO, and carried out primarily by IRTF telescope operators D. Griep, W. Golisch, and P. Fukumura–Sawada. Some of the images are published on the International Jupiter Watch website.[31]

The IRTF images are made using five narrow-band filters, as follows (Figures 9, 10 & 11).

- At 1.58μm: Near-IR continuum, comparable with the ~0.8μm I-band; detects sunlight reflected from deep clouds, sensitive to cloud particle albedos. However there is some methane absorption so this wavelength may not probe quite as deeply as 0.8μm light. In the equatorial region it resembles the 3.78μm picture.
- At 2.30μm: The strongest methane band, showing sunlight reflected from the stratospheric hazes, at the 100-mbar level and above.
- At 3.53μm: The planet is virtually black, except for $H_3^+$ emission from aurorae near the poles.

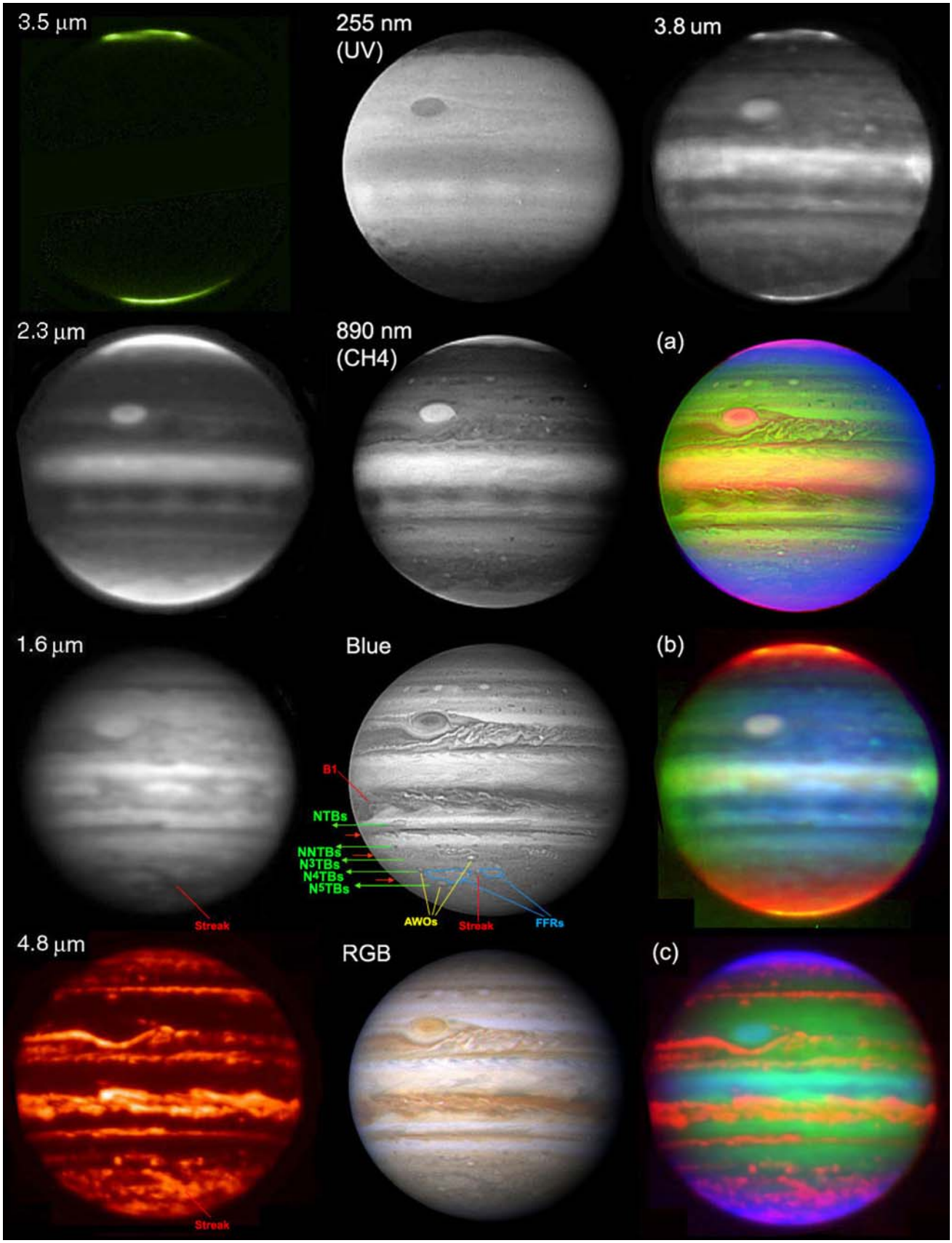


**Figure 10.** Complete sets of images from IRTF (Oct 5, first column) and *Cassini* (Oct 8, middle column). Wavelengths are marked. The GRS is at upper left. On the NEB, note the methane-dark and UV-bright waves, including the most intense one on the p. limb p. barge B1. On the *Cassini* blue image are marked dynamical features of the far northern regions: jetstreams (approximate positions; note jetstream spots on NTBs and NNTBs); anticyclonic white ovals (AWOs; the southernmost is NNTC no.6); folded filamentary regions (FFRs). A large streak, dark from red to 1.6μm and bright at 4.8μm, is revealed as a clear space between FFRs. In the right-hand column are three false-colour composites (by JHR):

(a) *Cassini*: Blue= 255nm UV (negative), green= blue light, red= 890nm methane band.
(b) IRTF: Blue= 1.6μm, green= 3.8μm, red= 2.3μm.
(c) IRTF: Blue= 2.3μm, green= 1.6μm, red= 4.8μm.

– At 3.78μm: A mixed waveband, with weak methane absorption but other unique features, detecting sunlight reflected from particles at the 1-bar level and higher. These images are complex but often weirdly beautiful, largely a mixture of near-IR continuum plus methane-bright hazes, plus some unique bright atmospheric spots, and $H_3^+$ auroral emission near the poles. The bright atmospheric spots are abundant in the EZ and SEB and STropZ, often located on the p. edges of dark spots running p. or f. on jetstreams, but also in other places. They seem to be high-altitude clouds that fail to reflect at shorter wavelengths, perhaps because they are made of larger particles.
– At 4.78μm: Thermal emission from deep in the planet; it is absorbed by the tropospheric clouds, which therefore appear dark, silhouetted against the deeper glow. So it is generally a negative of the visible-light image, or more particularly of the 1.6μm image; this is consistent with both wavebands sensing clouds slightly deeper than the main visible clouds. However in the equatorial region, a 4.78μm image is more like a visible image, suggesting that the relevant opacity levels are different there.

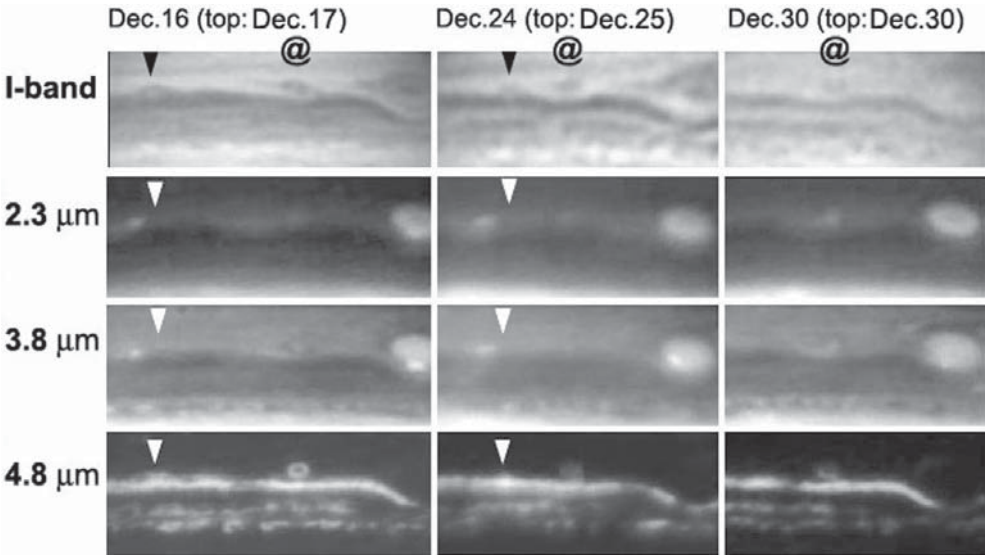


**Figure 11.** Interaction of a SEBs jetstream spot (arrowhead) with the little brown oval (STropC no.4:@) p. the GRS (seen at right). A methane-bright cloud trails behind the retrograding jetstream spot. The brown oval is only slightly methane-bright, but on Dec 30 when the two spots are in contact the methane-bright cloud envelops the complex. Top (I-band) images are on Dec 17 (Jesus R. Sanchez, Spain), 25 (Jesper Sørensen, Denmark), and 30 (Antonio Cidadão, Portugal). Other images are from IRTF on Dec 16, 24 and 30.

# General appearance of the planet in multispectral images, 2000/2001

This section reviews the general appearance of the planet in these multispectral images in 2000/2001. Most of the appearances are thought to be typical, although some have not been well documented before. The two special phenomena – the NEB waves and the SED– are described in a separate section below, and Paper III.

Each region is summarised from amateur and IRTF images, with comments from the few publicly-released *Cassini* images where significant. Unless otherwise stated, the appearances in 2000/2001 are typical.

## Southern hemisphere

*S. and S.S. Temperate regions*

– Visible: The belt/zone pattern as described in Paper I.
– Methane: Generally low contrast in the region. The little anticyclonic white ovals (AWOs) at 41°S are methane-bright at 0.89μm (*Cassini*) and at 3.8μm, and weakly so at 2.3μm.
– 4.8μm: Some very bright little spots and belt segments, representing a subset of the visibly dark structures. The little AWOs are dark but most have bright rims.

*Oval BA (Figures 12 & 16)*

This is the archetypal AWO, covered with high-altitude cloud.

– Mid-UV (*Cassini*): A very dark oval with bright rim.
– Visible, I-band, 1.6μm: Large but low-contrast oval, with an incomplete dark rim.
– Methane: Very bright oval.
– 4.8μm: All dark, with no rim.

*Great Red Spot (Figures 9, 10 & 11)*

This largest anticyclonic oval on the planet is characterised by thick clouds and thick high-altitude reddish haze. (Also see images in ref.10.)

– Mid- and near-UV: The darkest feature on the planet, along with the NEB.
– Visible: As usual, the oval contains orange colour mainly in a dark central condensation; it has a grey-brown oval rim, and a darker grey outer rim that varies.
– I-band, 1.6μm: Bright, with dark outer rim.
– Methane: The whole oval very bright, as usual.
– 4.8μm: Dark, with variable bright rim representing the outer rim and Red Spot Hollow, as usual.

*STropZ*

A bright zone from UV to IR, as usual, except for the transient dark STropBand.

*Spot in STropZ: (Figures 9 & 11)*

This small oval p. the GRS (STropC no.4 in Paper I; L2 ~ 30, L3 ~ 345) is of special interest. It has existed since 1999, and was a strong anticyclonic oval, even though it was not specially red in the visible range. It resembles a similar spot which merged with the GRS in 1997.[32–34]

– Near-UV: Low-resolution image [Akutsu, Dec 15] reveals the spot to be dark.
– Visible: A small brown spot; revealed by *Cassini* to be an anticyclonic ring (Figure A2 of Paper I).

**Table 2. Latitudes (zenographic)**

| | *Visible (Paper I)* | *I-band 0.8μm (Akutsu)* | *Methane 0.89μm (Akutsu)* | *Methane 2.3μm (IRTF)* | *1.6μm (IRTF)* | *3.8μm (IRTF)* | *Thermal 4.8μm (IRTF)* |
|---|---|---|---|---|---|---|---|
| Oval BA | –32.2 | | –31.7 | –31.2 | | | |
| SEBs | –20.6 | **–21.8** | –21.1 | –19.8 | **–21.6** | **–21.2** | –20.7 |
| SEBn | –8.0 | –7.4 | *–5.6* | *–3.55* | *–3.8* | *–3.8* | –7.0 |
| | | | [~–7]* | | **–9.4** | **–9.4** | |
| NEBs | 8.5 | 8.7 | ~8.9 | **(~9)** | **9.1** | **9.1** | 8.2 |
| | | | to **~11.0** | (v. diffuse) | | | |
| NEBn | 20.5 | 19.9 | *18.7* | *19.1* | 19.9 | 19.9 | 19.7 |
| NTBs | 25 | 24.8 | 24.8 | *22.5* | 24.6 | 24.3 | 24.6 |
| NTBn | 28.2 | 28.6 | **29.4** | **31.5** | **29.1** | **29.1** | 27.7 |

Latitudes (zenographic) were measured on 6 sets of Akutsu's images on 2000 Dec 14 and 29, and on 6 sets of IRTF images on Dec 29 and 30. Standard deviations were 0.7° or less.
The first column gives mean latitudes for the apparition in visible light from Paper I; IR latitudes are printed in bold if significantly higher, in italics if significantly lower.
Boundaries marked ~ were diffuse or irregular.
For SEBn, these were longitudes that did not involve the SED main complex, except:
*Value of ~–7° is for very diffuse SEBn just f. the main complex. At 1.6 and 3.8μm, –3.8 and -9.4° are for N edges of separate 'belt' components.
In addition the following latitudes were measured on the 6 IRTF images at 2.3μm for the edges of the bright polar hoods: SPH, –63.7 (±1.1); NPH, +64.6 (±1.5) for the brightest part, with very diffuse haze extending down to +50 (±3.5)°

– I-band, 1.6μm: Pale dusky spot, or ring [IRTF, Dec 16].
– Methane: At 2.3μm and 3.8μm, bright in the autumn [Sep, Nov], still just detectable in Dec. Some of this brightness may arise from interactions with jetstream spots (e.g. Figure 11). (Not detected in amateur images.)
– 4.8μm: Fairly bright; in the autumn, this was a rim slightly S of the methane-bright part, but in Dec it was a complete bright ring.

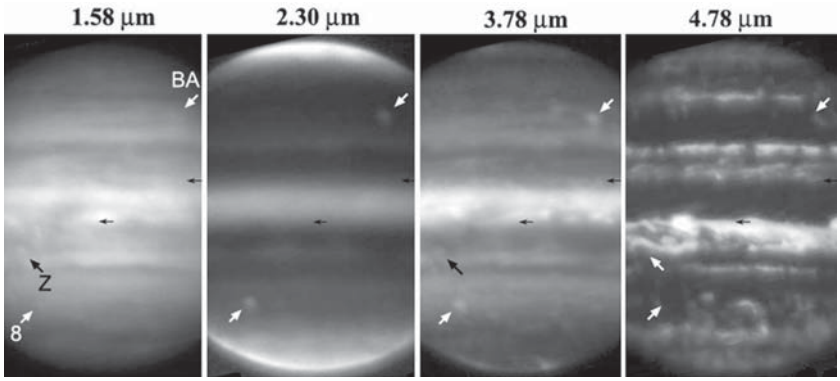


**Figure 12A.** Set of IRTF images showing how the belts in each waveband are aligned. Dec 29, centred around 09h23m UT, CM3=209.5. Three AWOs are arrowed: oval BA and NNTC no.8 are methane-bright but do not have bright rims at 4.8μm; white spot Z (in contact with a NTBs jetstream spot) is not methane-bright but does have a partial bright rim at 4.8μm. Compare with visible colour 'Millennium Map' in Paper I.

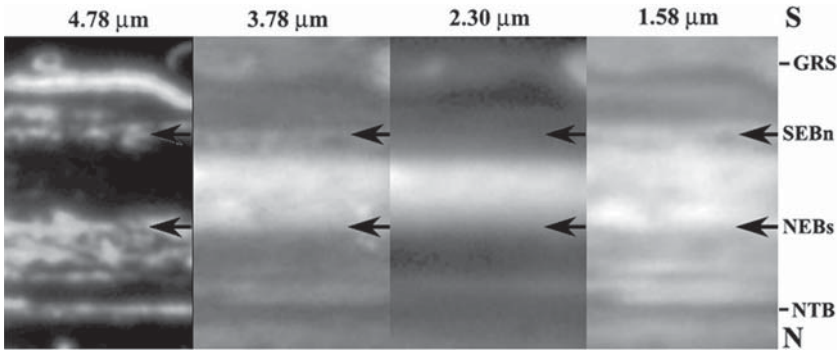


**Figure 12B.** IRTF images showing the alignment of NEBs and SEBn belt edges. Dec 30, centred around 10h08m UT, CM3=26. The GRS is at top right and STropZ brown oval at top left. While the boundaries at 4.8μm agree with visible light, boundaries in other IR wavebands are slightly different. Arrows indicate the most discordant latitudes, approx. 8°S and N.

### *SEBs (with jetstream spots)*

SEB(S) is dark at all wavelengths from UV to IR. Retrograding spots are densely crowded, though they do not have well-defined shapes; the images show that they are largely free of clouds at all levels.

– Visible: Jetstream spots are dark grey. The *Cassini* movie shows their motion very clearly, and their anticyclonic circulation as two of them merge.
– I-band, 1.6μm: Jetstream spots are very dark, extending further S. than in the visible (Table 2).
– Methane (0.89μm): Also very dark spots, though some differences from I-band.
– Methane (2.3μm): S. edge of spots is masked by lighter STropZ.
– 3.8μm: In addition to the dark belt and spots, there are several tiny bright spots, including the one shown retrograding in Figure 11 which was on the f. edge of a dark jetstream spot.
– 4.8μm: Jetstream spots are very bright streaks, comprising the brightest part of the SEB.

### *SEB*

– Near-UV: Dark belt.
– Visible: SEB(S) is very dark, dull brown. The SEBZ varies from bright yellowish-white to dull yellowish-brown. There is a long bluish northerly SEB(C) sector p. the RSH, and elsewhere a grey-brown SEB(N) which is weak and disturbed by the SED.
– I-band: Most of SEB resembles the visible picture, but much of the SEB(N) is faint or absent due to the SED. At 1.6μm, SEB(N) is quite dark though discontinuous.
– Methane: The whole SEB is very dark. (However, the cores of the bright plume-heads in mid-SEB f. the GRS are sometimes methane-bright, not only in amateur images,[3] but also in the highly methane-selective images from *Galileo*[19,20] and *Cassini*[21] – well shown in Figure 4.)
– 4.8μm: SEB(S) is very bright, narrow SEBZ totally dark, SEB(N) composed of moderately

bright streaks, fragmentary (especially disrupted p. the SED main complex, but bright just f. the main complex).

## Equatorial region

*SEBn/EZ(S)*

The South Equatorial Disturbance (SED) dominated these latitudes; full details will be given in Paper III. In summer 2000, the visible disturbance covered more than half the circumference; thereafter, it faded away until little was visible. However, hi-res images revealed that smallscale disturbance still affected most of the circumference, and extensive disturbance remained in the infrared. The main complex remained a striking feature in methane bands. The stormy sector is shown in Figures 2, 4–6, 18.

Unusual mismatches between wavelengths were shown in two narrow bands: ~8-9°S (SEBn) and ~5-7°S (EZs), which resemble the anomalous NEBs and EZn respectively (see below), in that the 1.6 and 3.8μm images show the opposite pattern to what is expected. (See Figures 11, 12A, 12B and Table 2.)

- Near-UV (lo-res): No disturbance visible.
- Visible: White, except for the 'stormy sector' which was still extensive in summer 2000; thereafter disturbance on a smaller scale with only a few large bluish streaks and patches interrupting the largely white EZ(S).
- I-band, 1.6μm: In the stormy sector, the visibly bluish streaks and spots are very dark – a striking picture. Later, dark streaks and spots form a dark band in EZ(S), still down to 4°S, and present all around at 1.6μm.
- Methane: The undisturbed sector is bright at 0.89μm, but diffusely dark at 2.3 and 3.8μm; all wavelengths are increasingly dark with increasing longitude, so the stormy sector of SEBn/EZ(S) is all uniformly diffusely dark – like the tropical zones but unlike EZ(N).
- 3.8μm: A striking picture, combining the fine detail at 1.6μm with the diffuse large-scale contrasts at 2.3μm, plus a few bright spots. Particularly dark p. and around the main complex, presumably a mixture of albedo and altitude effects.
- 4.8μm: A negative of the visible but not 1.6μm images: SEBn bright and EZ(S) dark as usual. In the stormy sector there is a band of bright spots and streaks, often coinciding in longitude with the visibly blue and I-band-dark streaks, but not extending so far north – only down to 7°S.

*EZ(N)/NEBs*

The EB and festoons and many of the NEBs projections, all visibly prominent up to 2000 June, rapidly faded away in late 2000, leaving only seven typical NEBs projections and no EB. As usual, these projections/hotspots were dark at near-IR and long visible wavelengths, due to the absence of clouds within them, but pale in blue and almost undetectable in UV and methane, due to the high-altitude haze of the EZ overlying them. (Also see images in ref.10.) But between the projections, the NEBs (8–9°N) shows paradoxical properties in IR wavebands.

- Mid-UV (*Cassini*): EZ(N) all dark, being the negative of the methane picture.
- Near-UV (lo-res): EZ(N) slightly shaded, i.e. showing some enhanced absorption, consistent with the visible tint, but not nearly as dark as during coloration events in 1989/90 or 2001/02.
- Visible: Where still present, the NEBs projections are low-contrast in blue but very dark in red, hence their bluish-grey tint. As many of them have faded away, the EZ(N) has a feeble yellowish-brown (fawn) tint in most images – not a distinctive colour, but one which would intensify in the next apparition.
- I-band: The projections and festoons show up extremely dark, but only as long as they are also present in visible light. (It was the *Cassini* I-band movie which best revealed the extremely fast speeds of the NEBs and SEBn jetstreams [A. Vasavada, cited in ref.15]. This was probably because this light could penetrate below the cloud-tops, just as the *Galileo* Probe found speeds increasing as it descended.)
- 1.6μm, 3.8μm: The projections and festoons show up extremely dark; in addition, one can still see the dark festoons and EB and some additional projections in EZ(S), although they have faded away at visible wavelengths. However, surprisingly, the NEBs is bright: the EZ extends up to 9°N (see latitudes in Table 2, and Figures 5, 12A, 12B, 14).
- 3.8μm images also show the large-scale contrast of methane images, plus tiny bright spots which are almost always present on the p. edges of the dark NEBs projections. These do not reflect so very brightly at other wavelengths, but may be high-altitude cloud 'rafts' that were shown in similar positions in *Voyager*'s hi-res visible images.
- Methane: The NEBs dark projections are visible in Akutsu's 0.89μm images[3] (with an incompletely selective filter), but not in the *Cassini* 0.89μm images [Figures 4, 10 & 15] nor in 2.3μm images. The EZ(N) is all covered with a very methane-bright (high and thick) haze, as usual; EB and festoons are not visible. This haze extends some way over the NEB(S). In our images at 2.3μm and 0.89μm its boundary is diffuse, but hi-res 0.89μm images from *Cassini* [Figures 4, 10 & 15] and in earlier years from *Galileo*[3,10,51] show a sharp boundary well north of the visible NEBs. The situation was the same in 1999/2000.[3]
- 4.8μm: The visibly dark projections are the very bright hot-spots, conspicuous as usual. Their spatial extent is the same as in visible images, as is the boundary of the NEB. Where projections have disappeared, their bases are still evident as streaks in the NEBs which are bright at 4.8μm and dark bluish in visible light. The EZ is all dark at 4.8μm, with only faint fragments of festoons and no EB, showing that this radiation is blocked by clouds throughout the EZ.

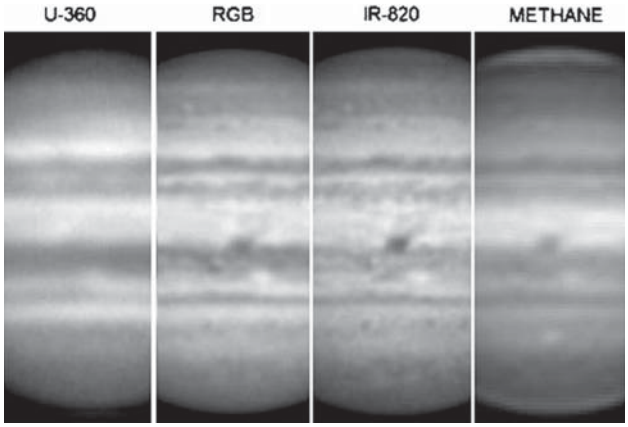


**Figure 13.** Set of images by Akutsu showing how the belts in each waveband are aligned: Nov 5, 14h 07–19m UT, CM2=203–210. NEBn white spot Z and NNTC oval no.8 are near the centre of each image, both bright in the 890nm (methane) image.

*Discussion: Models for NEBs and SEBn*

At most times, most areas of the equatorial region have straightforward structure. The EZ has thick cloud which reflects all wavelengths and is opaque to 4.8μm. Conversely, the visibly dark features (including long segments of NEB(S) and SEB(N), and projections and festoons into the EZ) are

largely clear to all wavelengths (except the strong methane wavelengths because of thick EZ haze covering them). However in 2000/2001, our images indicate anomalous cloud layers in at least three categories. They seem to be separable into (i) anomalies of the diffuse upper haze, sensed by strong methane bands, which show opposite deviations over NEBs and SEBn; (ii, iii) anomalies in or near the visible cloud layer, especially seen at 1.6μm and 3.8μm which are weak methane bands, which show similar deviations from expectation in north and south, being paradoxically bright in (ii) a narrow strip along the visibly dark NEBs and SEBn, and paradoxically dark in (iii) the typically bluish patches of EZ(N) and (S) (including the NEBs projections and festoons, and the dark patches of the SED) after they had faded at visible wavelengths. These properties all call for novel cloud layers with unusual properties; whether these are due to albedo, particle size, or density, is yet to be determined, but we offer some suggestions below.

(i) Upper haze. As seen at 0.89μm and 2.3μm, this thick and bright haze layer is also bright over NEBs (to ~9°N) but is deficient over EZ(S) (down to 4–6°S). In both sides, it is diffuse and uniform across the visibly dark patches. These anomalous methane patterns at least partly predate the visible whitening. The methane-bright strip on NEBs was already present in *Galileo* closeups in 1996 and 1999.[3,51] The methane-dark strip in EZ(S) was at least partly evident in *Galileo* closeups in 1996 Nov (C3 encounter), when the visually very bright strip of southernmost EZ was dusky at 0.89μm – although the adjacent SEBn was still darker [ref.51, and raw *Galileo* images]. So this was not entirely a consequence of the SED.

(ii) Visible cloud levels: NEBs and SEBn, coinciding with the prograde jets. There is a narrow strip (~8 to 9°N) between the NEBs boundary in visible and 4.8μm images, and the boundary in 1.6μm and 3.8μm images. A similar anomalous strip seems to exist in some sectors of SEBn (~8 to 9°S) although it is less definite as this strip is streaky and intermediate in intensity at all wavelengths. This implies a cloud layer which reflects at 1.6 and 3.8μm but transmits at 4.8μm and either transmits or absorbs at visible and I-band. Probably it is near the visible cloud-top level, because 1.6 and 3.8μm are weakly methane-sensitive, and because it would seem implausible for such an anomalous layer to lie between the 'well-behaved' visible and 4.8μm opacity levels (especially in a region subject to strong shear and disturbances). It could be a thickening of the lower levels of the methane-reflective layer that also overlies this strip.

(iii) Visible cloud levels: Visibly dark bluish patches which were progressively disappearing (filled in by white cloud) in late 2000. These included NEBs projections and festoons, the EB, and the bluish patches of the SED. From the *Galileo* Probe it is known that the NEBs projections, at least, are virtually cloud-free below the upper haze layer, i.e. from 0.4 bars down to at least 20 bars. The new white cloud blocks the visible, I-band and 4.8μm, but does not reflect at 3.8μm and 1.6μm, therefore it cannot simply be a thickening of the upper haze. It must be either transparent or absorbing at 1.6 and 3.8μm. The properties of this new white cloud could perhaps be explained without invoking differential albedo, if it is thick and low-lying, deeper than the visible cloud-tops of neighbouring areas; thus the persisting dark patches at 1.6 and 3.8μm could be explained largely by extra methane absorption. This arrangement, whereby the patches still have less cloud at visible cloud-top level, could be consistent with these weather systems still being maintained with a downdraft of vapour-free air.[14,15]

### *NEB*

The NEB was undergoing a classical 'broadening event'[1,5] in which the visibly dark belt expands northwards into the canonical NTropZ. This had developed slowly and in summer 2000 was still incomplete. As the apparition progressed, remaining 'normal' sectors of NEBn gradually darkened, until at the new year, the NEB was fully broadened at all longitudes.

At high levels, revealed in mid-UV and methane bands, the NEB displayed a remarkable pattern of large diffuse waves, which is discussed in detail in a subsequent section.

For images in December, and for alignment of belts in different wavebands, see Figures 6, 12A, 12B, 13, 14, and Figure A3 of Paper I.

- Mid-UV: Negative of the methane image (see below).
- Near-UV: NEB is the darkest belt, consistent with visible reddening.
- Visible: The broadening developed as described above. NEB was the reddest belt; this was not a strong colour but may represent the reddening that often follows a broadening event. (The reddening would become more conspicuous in 2001/2002.) The brown barges, though small, were very dark, and possibly redder than the main belt.
- I-band, 1.6μm: These also showed the broadening of the dark belt, but lagging behind the visible; in Dec–Jan it was still not complete. There was much spotty structure in the belt, with especially dark patches at 19°N including NTropC no.1a (yellowish-brown; Figures 2, 3, 9) and no.11 and the border around white spot Z (both grey in visible light; Figure 14 and Figure A3 of Paper I). In contrast, the barges are faint or invisible in I-band; indeed they cannot be reliably distinguished in any IRTF wavebands.
- Methane (0.89, 2.3, 3.8μm): The NEB did not broaden as much as in visible light, if at all (see latitudes in Table 2). The remarkable pattern of dark waves (described in a separate section below) spanned ~11 to 19°N, both before and after the visible NEBn edge extended from 17°N to 20°N. The dark waves were associated with the barges. However white spot Z was inconspicuous at all the IR wavelengths (Figure 14); these NEBn AWOs are not bright in methane.
- 4.8μm: This showed approximately a negative of the 1.6μm image, the belt being composed of many bright streaks. As at 1.6μm, the belt did broaden over time but lagged behind the visible, and the most intense features were grey patches in visible light.

### *NEB (Discussion)*

It should now be possible to begin analysing the nature of the NEB broadening event, as there has been hi-res multispectral coverage of broadening events in 1993, 1996, and 2000, which proceeded in somewhat different manners. The present event developed most completely at visible wavelengths, and followed on in I-band and 4.8μm. This suggests that the event may start with a thinning of the visible ammonia cloud layer, and only then propagate deeper, leading to partial breakup of the clouds at the 1–2 bar level.

Meanwhile the belt did not clearly broaden in methane bands, i.e. at the level of the high-altitude haze. In 2000, this discrepancy was confused by the dramatic wave pattern that developed; some of the large dark waves did indeed extend diffusely north over part or all of the NTropZ. But in sectors where the NEB was visibly expanded but without methane-dark waves, the belt was still of normal width in methane. This discrepancy also seems to be shown in the limited data available following previous NEB expansion events: in 1994 and

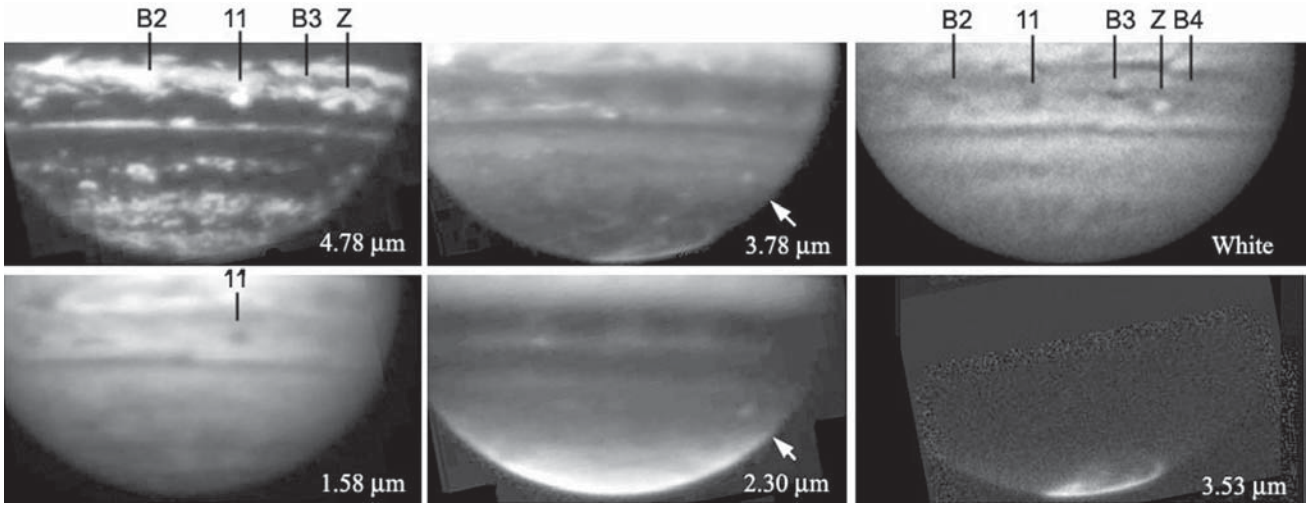


**Figure 14.** A set of IRTF images of the northern hemisphere on Dec 18, taken around 13h05m UT (CM2=152, CM3=128); and a white-light image by Jean Dijon (France) on Dec 19, 19h34m UT (CM2=178). Compare *Cassini* image Figure A3 in Paper I. NEB broadening is here complete in blue light but not at 1.6µm nor 4.8µm. This sector includes NEB barges B2 and B3, and the dark grey anticyclonic spot no.11, with white spot Z near f. limb. There is a fine pattern of methane-dark waves on the NEB, coinciding with these visibly dark spots and other projections at 1.6µm and 4.8µm. Also note the NNTZ methane-bright spot no.8 (arrowed near f. limb), and much detail in the north polar hood and aurora. (Also see false colour version Figure 5.)

1997,[3,35] when NEB was expanded in the visible, it was not fully expanded in the 0.89µm methane images. This discrepancy accords with other dislocations of the belt-zone pattern, such as fadings of the STB and SEB;[5] when the visible belt pattern temporarily changes, the methane pattern often does not. Thus, albedo changes in the visible clouds do not change the pattern of the high-altitude haze that overlies them.

However, an NEB broadening event is commonly followed by reddening of the belt, and this is thought to be due to increased violet absorption in the haze layer. Possibly this only occurs at the lower, denser levels adjacent to the ammonia cloud layer.

The pattern of large methane-dark waves was, however, a transient phenomenon in the high-altitude haze, which seems to have been associated with the conclusion of the NEB broadening event, as we discuss in a subsequent section.

## Northern hemisphere

### *NTBs jetstream spots: (Figures 9, 14, 15)*

At all wavelengths, the NTBs 'humps' appear typically belt-like, i.e. deficient in clouds at all levels. They consist of NTB material stacked up against the true jetstream spots which are low-contrast anticyclonic rings, as revealed by HST and *Cassini* [refs. 36, 37, and Paper I).

- Visible: Indistinct long humps or steps.
- 1.6µm: Very dark.
- 2.3µm: Not visible. (The NTB is much broader than in visible light; Table 2.)
- 3.8µm: Dark, sometimes with a bright cloud fleck on the p. edge [Figure 14].
- 4.8µm: Very bright.

### *NNTZ anticyclonic oval: (Figures 12A, 13, 14)*

For many years there have typically been two methane-bright spots in the NNTZ latitudes, coinciding with anticyclonic ovals which are sometimes visibly red. In 2000/2001 there was just one of these (NNTC no.8; see Paper I).

- Mid-UV (*Cassini*): A very dark oval.
- Methane: Bright in all methane wavebands.
- Visible: A pale light oval, so difficult to image. A *Cassini* image (Figure A3 in Paper I ) shows that it is a well-formed light anticyclonic oval with a reddish core, typical of methane-bright spots.

### *North Polar Region: (Figures 10 & 14)*

The visible clouds are overlain by the North Polar Hood, within which remarkable structures have been reported by HST and in mid-IR.[27,38] This is in turn surmounted by the auroral oval.

- Mid-UV (*Cassini*): The N. Polar Hood is dark, and very extensive, down to ~45°N, and shows lots of small-scale patchy structure. A *Cassini* 'polar projection movie' has recorded the origin of a huge dark oval at ~60–70°N within it, beneath the aurora.[21,26]
- 2.3µm: The very bright N. Polar Hood extends down to 65°N (further at the limb where it is brightened), and it has a very diffuse extension down to ~50°N. It shows diffuse irregular largescale mottling, unrelated to the structures at other wavelengths.
- 1.6µm and 3.8µm: Many dark spots, both small-scale and large-scale. On one side of the planet there are just innumerable small spots; on the other side, remarkable large-scale light patches and dark streaks, looping irregularly around the NPR (Figure 10). At 3.8µm, the aurora shines brightly.
- 4.8µm: Many dark spots, both small-scale and large-scale, largely a negative of the 1.6µm pattern. The 1.6µm dark streaks are bright at 4.8µm, though usually broken into smaller patches.

### *North Polar Region (discussion)*

The large-scale dark streaks and loops seen at 1.6µm and 3.8µm are not obvious at visible wavelengths. However they are probably similar to the large dark patches noted in the NPR in 1997 by the ALPO in the first amateur I-band images [cited in ref.34]. They cut across the jetstream latitudes. They appear to be a previously unreported type of structure.

Their meteorology can be inferred by comparing IRTF images with *Cassini* images (e.g. Figure 10). The most distinct large light areas in the 1.6µm images coincide with large cy-

clonic folded filamentary regions (FFRs) in the N$^4$TB domain in the blue-light *Cassini* images. This domain also contained very large FFRs in *Voyager* images, some of them extending across the jetstreams (e.g. p.94 of ref.5). FFRs in the N$^4$TB domain also produce more lightning than anywhere else on the planet, according to *Voyager* and *Galileo* imaging.[39–41] The 1.6μm light areas further north are not resolved in the early *Cassini* images but may well be similar FFRs.

The dark streaks and loops at 1.6μm, which are bright at 4.8μm, are presumably regions of less disturbed and largely clear atmosphere between the FFRs. They are less evident at visible wavelengths because a diffuse haze overlies the NPR. They span multiple domains because there are no visibly bright zones in these high latitudes, just scattered anticyclonic white ovals.

## The wave pattern over the North Equatorial Belt

In 2000/2001, methane-band images revealed a striking wave-like pattern of large diffuse dark patches overlying many longitudes of the NEB, spanning ~11–19°N. The most conspicuous dark patches were aligned with visible features, but many did not have obvious visible partners; instead they formed a regular series of waves with wavelength 20–24° longitude. These waves were shown in all methane bands, both at 0.89μm by amateurs and by the *Cassini* spacecraft, and at 2.3μm and 3.8μm from the IRTF. These wavebands sense high-altitude haze lying above the visible clouds, in the upper troposphere, so the waves appear to be thinnings in this haze. They were also shown as diffuse bright patches in the mid-UV images by *Cassini*, indicating that they probably extended into the stratosphere.

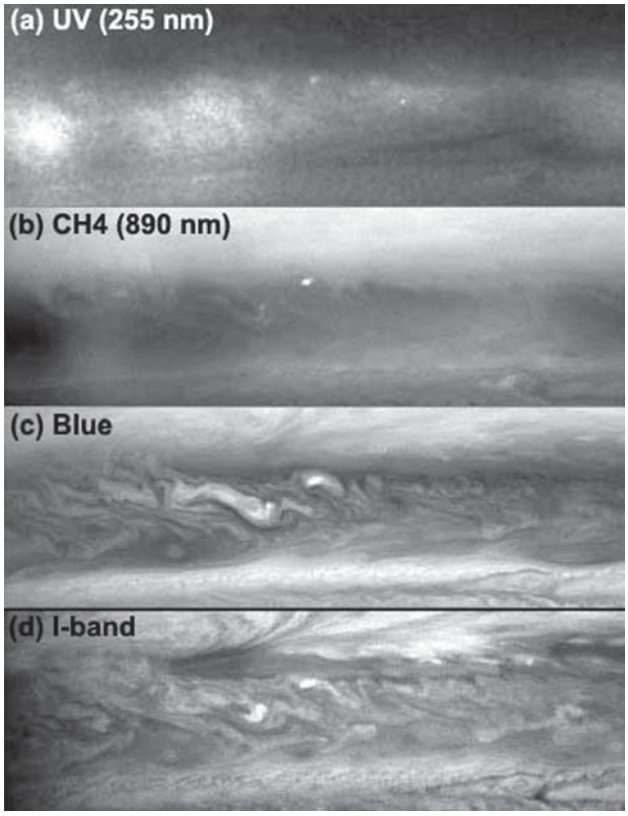


**Figure 15.** *Cassini* closeups of the NEB, at 4 different wavelengths on Nov 27. This covers the region between barges B5 (temporarily obscured by rifts, i.e. the turbulence in the left part of the frame) and B6. Diffuse waves are prominent at left and right, south of regions with anticyclonic recirculation on NEBn. Within the bright 'rifts' are several small bright spots which are energetic convective storms like those in the SEB [Figure 4]. The *Cassini* team point out that one in the center of the frame is bright even in the UV image, implying that it extends exceptionally high. They suggest that it may resemble giant thunderstorms on Earth which can erupt all the way into the stratosphere. There is a NTBs jetstream spot in the lower right corner. From the *Cassini* website.[26] *NASA/JPL/University of Arizona.*

The wave pattern is well shown in Figures 2, 9, 10, 12A, 14, 15 and 16. The hi-res *Cassini* images (Figures 10 & 15) show that the methane-dark waves are genuinely large and diffuse, and distinct from (though associated with) the visible features such as dark barges. The wave pattern has recently been described by the *Cassini* imaging team.[21,26]

We have measured these diffuse dark patches on all the methane images in 2000/2001, both the amateur images at 0.89μm (mostly by Akutsu, some by Colville and Cidadao), and the IRTF images at 3.8 and 2.3μm. There were similar numbers of images from Akutsu and from IRTF, and all of them were needed to give a complete view. Images were measured manually; more precise methods could be used, but this is sufficient given the large scale and diffuseness of these patches.

The measured longitudes are plotted in Figure 17, and the drift of each patch is listed in Table 3. Also plotted on Figure 17 are the tracks of the visible dark barges (numbered B1 to B6) and two anticyclonic white ovals (NTropC no.5 and white spot Z; see Paper I). It is obvious on the chart, and on many individual images, that the waves were often associated with the barges. However the waves could not be confused with the barges themselves: the barges were much smaller, and faint or invisible in near-IR (e.g. Figure 14), and usually located at the f. edges of the methane-dark waves.

The largest and darkest wave lay on the p. side of barge B1. Waves also lay on the p. sides of four other barges, including B3 and B5 whose waves also became very large later in the apparition. Between barges B1 and B2, a strong array of waves was evident for most of the apparition. Less stable waves appeared at times between the other barges. The chart shows that the waves moved with speeds identical to those of the visible features underlying or flanking them, and that on three occasions when the visible pattern was disrupted, a wave appeared or disappeared accordingly.

### The waves over the NEB: detailed description

The phenomenon will next be described in detail by dividing the NEB into three sectors:

a) from B1 to B2; irregular NEBn edge in 2000; broadening completed around the end of 2000.

b) from B2 to B5; includes B3 and w.s.Z; broadening completed around the end of 2000.

c) from B5 to B1; fully broadened before the apparition began. There was an especially conspicuous patch associated with barge B1.

**Table 3. NEB methane-dark patches, 2000/2001**

| *No.* | *L2(O)* | *DL2* | *Dates* | *Notes* |
|---|---|---|---|---|
| 1 | 30 | –4.2 | Aug 28–Dec 29 (Mar 8) | B1 at f. edge. V.long, v.dark. Coincides with visible brown cloud. |
| 2 | 66 | 0.8 | Sep 14–Dec 1 | |
| 3 | (87) | 1.3 | Sep 14–Nov 15 | (Disapp. when w.s.no.5 retrograded) |
| 3b | (79) | 1.3 | Dec 15–Jan 26 | |
| 4 | 100 | –1.4 | Sep 19–Jan 26 | At small dark spot no.7 (new barge B8) |
| 5 | 122 | –3.2 | Sep 19–Jan 11 | |
| 6 | 146 | –4.2 | Sep 19–Jan 26 | B2 at f. edge. |
| 7 | (167) | [–4] | (Oct 5) Dec 4–Jan 26 | At dark grey spot no.11. |
| 8 | 189 | –6.9 | Nov 24–Mar 6 (Oct 5–Apr.26) | B3 at f. edge; V.dark and long after Jan |
| 9 | 208 | [nd] | Nov 29–Dec 29 | |
| 10 | 231 | [–4]v | Nov 10–Jan 2 | At minor barge B4 |
| 11 | 257 | –3.1 | Aug 27–Mar 7 | B5 at f. edge. V.dark, becoming v. long. Coincides with visible dusky cloud. |
| 12 | 282 | [–1]v | (Aug 27) Oct 7–Feb 24 | |
| 13 | (304) | [nd] | (Aug 27) Dec 7–Feb 7 | B6 at f. edge. |
| 14 | 358 | [nd]v | (Sep 14–Jan 12) | (Not a continuous feature.) |
| 15 | (367) | [–5] | Oct 4–Nov 4 | |

L2(O), System II longitude at opposition on 2000 Nov 28. (For L3(O), subtract 30.0°.)
DL2 in degrees per 30 days [In brackets if imprecise; nd, not determined; v, variable].
(For DL3, drift in System III longitude, add 8.0°/month.)

### *The B1 patch (L2~40–>20): (Figures 2, 9, 10, 16)*

This was the biggest methane-dark patch for most of the apparition. It was present by August 28; already big and northerly by Sep 14; vast and very dark in Oct; 25° long in Nov–Dec. It extended right across the NTropZ, at least from Oct 4 to Dec 29 (IRTF).

Its f. end was always marked by the little barge B1. The longitudes of the dark wave covered a region where there was evidence for anticyclonic circulation Np. B1 at ~19°N (Paper I), viz. the prograding spot (NTropC no.1a) and dark bulge into NTropZ (no.1b), which marked the f. end of the fully-expanded NEBn. (See the *Cassini* closeup in Figure A2 of Paper I.) This area Np. B1 gradually darkened from Sep to Dec, forming a large diffuse dark orange-brown cloud, which approximately coincided with the methane-dark wave.

At 4.8μm, the same NEBn bulge or cloud was notably bright (Figure 9), but did not cover the NTropZ.

This complex was very conspicuous in all wavebands up to late Dec. However by Dec 29 and Jan 12, the visibly dark cloud and 4.8μm bright spot had merged into the rest of the NEB and was not conspicuous; the expanded NEB was now continuous visually. The methane-dark patch was still long and dark, but less distinct from Dec 30 to Jan 12, and becoming lost in a long dark uneven stretch of NEB on Jan 13 (IRTF). However it was recorded again in early March (Figure 18).

### *Sector (a) from B1 to B2 (L2~50–150): (Figures 2, 9, 10, 16)*

This sector had a ragged NEBn edge in visible light, not fully expanded till late December, and it usually had the most distinct and obvious methane-dark waves.

Initially there were methane-dark patches at barges B2 (July 21) and B1 (Aug 28), but no other waves yet. The first images to span the sector between B1 and B2 (Sep 14 & 19; Figure 2), showed the classic wave pattern for the first time. This pattern persisted unchanged until mid-Nov. However the drifts of each dark patch were not uniform: while the waves at B1 and B2 had negative DL2 concordant with the visible barges, the four intervening waves were more stationary in L2, as were the visible features in the same L2 range (Figure 17 & Table 3). Most strikingly, one wave disappeared when an AWO (NTropC no.5) began retrograding across its longitude in Nov. This was a clear illustration that the methane-dark patches were constrained by the visible features.

After Dec 1, the wave pattern throughout this sector became unstable, probably because there were still conflicting motions in the underlying troposphere. There were some regular waves in Jan, but in Feb there were only indistinct waves or none at all throughout this sector.

### *Sector (b) from B2 to B5 (L2~150–260): (Figures 12, 14, 16)*

This was the sector containing white spot Z, which may disturb currents nearby (see Paper I and previous apparition reports). The sector did not complete the expansion until the end of 2000, as the yellowish strip around w.s.Z gradually darkened (Paper I). Waves at B2 and B5 were present in late July, but waves did not develop f. B2 until early Oct. Even these were inconstant until Dec, and there was still nothing between B3 and B5.

The methane-dark patch between B2 and B3 (re-)appeared on Dec 4, and this coincided with an interesting small spot at other wavelengths in Dec (NTropC no.11). We tracked it oscillating in the longitudes between B2 and B3. It was extremely dark at 1.6μm and extemely bright at 4.8μm (Figure 14), so it was a very deep hole, but anticyclonic. In visible colour, a *Cassini* closeup (Figure A3 in Paper I) showed it as a dark 'cold grey' anticyclonic ring.

Meanwhile in Nov, w.s.Z had prograded to only 12° f. B3, and a new small cusp or barge developed f. it (Figure A3 in Paper I). Thus w.s.Z no longer interrupted the wave pattern. The new barge (B4b) was the locus of a new methane-dark wave, one of two new ones which then completed the wave series around the planet. The methane wave pattern here was striking from Nov 29 to Dec 4 (Figure 16), but less regular from Dec 14 onwards. (The B5 patch was temporarily absent on Dec 7 & 9 (Akutsu), when B5 was also invisible, apparently masked by a passing rift.)

Some waves persisted to Jan 24–26, including B2, B3 (very long), and B5 (long, and still the centre of a nice wave array).

In Feb, only long indistinct dark sectors were seen, including the B3 and B5 waves. On Mar 6 & 7 (IRTF) the waves at B3 and B5 were both big and very dark and spanned NTropZ – like the wave at B1 earlier. The B3 wave was still similar in the last good image on April 26 (IRTF).

### *Sector (c) from B5 to B1 (L2~260–20): (Figures 9, 15)*

This was the sector that was already fully broadened in 2000 July. The methane-dark patches associated with barges B5 and B1 may have been present in the earliest images, and were definitely present from Aug 27–28 onwards; each was an especially large dark wave with the barge at the f. end. A dark patch at B6 had also appeared by Aug 27, though this was not a persistent feature. Otherwise, there were few if any methane-dark waves in this sector until September.

By Sep 14, the classic wave pattern was seen for the first time in this sector, but it was not stable. The wave pattern was absent on Sep 21–24, present on Oct 7 & 15, absent on Oct 22 & 27, present again on Nov 3–5. (This sector was not well observed for the rest of Nov.)

In Dec the regular pattern of waves was present throughout the sector, giving a continuous series all round the planet. It included the very long and/or dark waves associated with B5 and B6. But it was still not as distinct as in other sectors, and had become less regular again by Dec 29. In Feb, dark 'waves' were longer and less regular than before. Some were still present on March 8 (IRTF).

### *Late in the apparition*

The most conspicuous waves, in the sector L2~350–150, disappeared rather rapidly between mid-Dec and early Feb. Even the biggest one, at B1, became indistinct in Jan, though it was visible again in March (Figure 18). Likewise in the other sector, L2~150–350, after Jan, most waves disappeared; in Feb there were only indistinct dark waves and, most strikingly, several long very dark masses, especially those p. B3 and B5. Lo-res images in April (Cidadao) and May 1–4 (IRTF) still showed some NEB methane-dark patches but they were difficult to define on the planet's small disk.

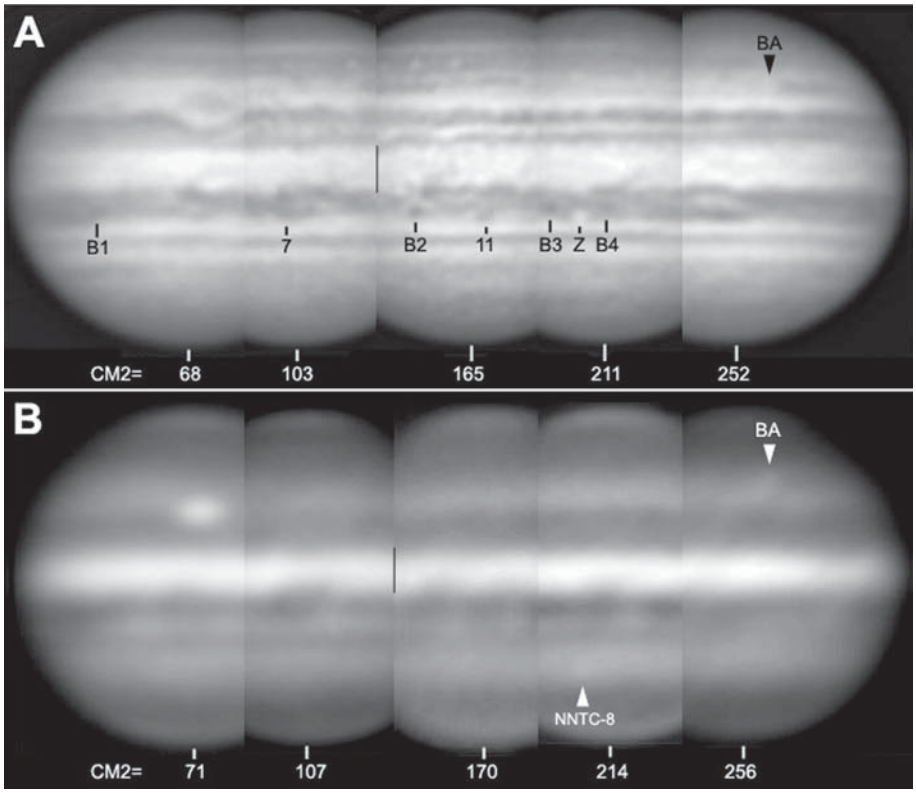


**Figure 16.** Sets of images by Akutsu on Dec 1 (first two disks) and Dec 4 (last three disks). CM2 is given below. Vertical line in EZ marks the join where a sector of System I longitudes is missing. (A) Visible colour (RGB); NEB barges and other spots are labelled as in Paper I. (Barge B5 is temporarily obscured by rifts.) (B) Methane (0.89μm); NEB waves are conspicuous across all the longitude shown. Two methane-bright AWOs are also labelled (oval BA and NNTC no.8).

## The waves over the NEB: discussion

*Spatial and temporal extent of the waves*

We have documented diffuse high-altitude waves over the NEB, seen in all methane absorption bands, and also by *Cassini* in mid-UV. From 2000 Sep to Dec, they constituted long unbroken series of waves spanning more than 180° longitude. Thus from Sep 14–19 the series consisted of 10 waves, wavelength 20.3°; from Dec 1–7, 12 waves, wavelength 23.5° . Over the whole apparition, the mean wavelength was 22.5°, equivalent to 16 waves around the planet.

The mean drift was DL2= –2.6°/mth (DL3= +5.4°/mth), essentially the same as for the visible dark barges.

These waves were probably a temporary phenomenon. They were most prominent and regular from 2000 Sep to 2001 Jan, and apparently less so before and after (even allowing for lower resolution of images). As a classical NEB broadening event was just coming to completion at this time, it seems possible that the wave pattern was a temporary consequence of it.

Indeed, the sector which was already fully broadened, in maps in 2000 Aug and Oct, extended from just f. w.s.Z to just p. B1, and this was the sector which usually had few or inconspicuous methane-dark waves (although curiously it had a prominent set from Dec 1–19 only). Conversely the waves were most prominent and stable in the sector from B1 to B3 inclusive, where broadening was not completed until Dec – and it was just then, in Dec and Jan, that the waves became indistinct.

*Where did the waves originate and propagate?*

The most important questions are: At what level did these patches originate, and at what level did they propagate as a coherent wave-train? Did the waves originate and propagate in the stratosphere or upper troposphere, where they were observed; or in the visible cloud layer; or even deeper?

It was evident in many images that the waves coincided with visible features, notably the small barges and cusps on NEBn. So first we need to ask: What was the relationship of the methane-dark waves to the visible features in the NEBn?

The dark waves were centred just p. the barges. At these locations, dark NEB material tends to be recirculated anticyclonically, forming evanescent dusky streaks and sometimes stable brown anticyclonic ovals. This was recorded in *Voyager* images in 1979[5] and in visible light images in 1999/2000.[36] In 1999/2000, a 'Little Brown Spot' was observed to form in this way; initially it was notably orange, and later the area spanning the spot and the barge f. it was a methane-dark patch.[3,36] The dark patches or waves associated with barges in 2000/2001 seem to represent exactly the same phenomenon (Paper I). This was most evident for the largest methane-dark patch, p. barge B1, where there was a large dark orange-brown cloud; but it probably held on a smaller scale for others.

More detail is shown in the *Cassini* images, especially Figure A3 of Paper I, which includes a diagram of the circulations. This image spans the locations of four strong methane-dark waves (Figure 14), and all these can be seen to be centred near anticyclonic circulation. In three cases this is irregular (just p. barges B2 and B3, and at the newly-forming little barge B4b); at each of the barges there are beautiful streaks strongly confirming the impression that brown belt material is whipped Np. from these locations to prograde in the darkened NTropZ. In the fourth case there is a tightly closed anticyclonic circulation (the deep grey spot, no.11). Also, all four locations are northward extensions of the NEB, bright at 4.8μm (Figure 14).

What about places where the high-altitude waves did not coincide with any major visible feature? Inspection of several hi-res images from IRTF and from *Cassini* suggests that there were indeed tropospheric undulations present (Figures 10 & 15). The waves do generally seem to be where the visibly-dark or thermally-bright (4.8μm) material of the NEB projects furthest into the NTropZ, even if these cusps would not otherwise have appeared substantial enough to attract attention.

But these various barges, etc., did not obviously comprise a regular wave pattern in visible light. Why then did the waves appear so regular at the higher level? In principle, the wave

pattern could develop at or below or above the visible clouds; each of these three hypotheses will be considered in turn.

*Hypothesis (i):* That in the visible clouds, there is indeed a tropospheric wave pattern with a wavelength of 20–25°, arising from meanderings of the retrograding NEBn jet. Both theoretical arguments and *Voyager* observations (reviewed on pp.265 & 273 of ref.5) suggest that the NEBn jet runs at its maximum possible speed, and when extra energy is fed into it, as during an outbreak of cyclonic rifts or a NEB broadening event, the jet begins to meander and discards energy into eddies on either side – these eddies becoming the cyclonic barges and anticyclonic ovals. The wavelength of 20–24° is just the minimum spacing that barges or ovals adopt in these circumstances when they are most numerous. Therefore it is plausible that the NEBn jet does spontaneously meander with this wavelength, and even where there are no visibly conspicuous circulations, there may be some slight undulation that affects recirculation into the NTropZ.

The idea of vertically propagating waves above the NEBn jet has already been advocated[42,43] to explain thermal waves, which appear to be the same phenomenon (see below). These were interpreted as stationary Rossby waves which can rise above the retrograding jet. They could be associated with small (~1°) latitudinal fluctuations of a jet, amplified at higher altitudes due to 'vortex stretching'.[43] So this mechanism is both observationally and physically plausible.

*Hypothesis (ii):* That the wave pattern originates below the visible clouds; it may not be fully manifest at the visible level, but it propagates temperature disturbances upward so that they can be revealed above the clouds. This was the hypothesis of Magalhaes *et al.*[44,45] We see no evidence for such a wave pattern in the 4.8μm images, although this may not rule it out.

*Hypothesis (iii):* That the wave pattern develops above the visible clouds, with only the initial disturbances imposed by major tropospheric circulations. In that case, although major dark patches could remain associated with barges, one would expect the intervening wave pattern to have a distinctive phase speed. However there was no sign of any such phase speed different from the speed of the underlying visible features.

The most striking evidence that the waves are individually controlled by the visible cloud circulations, as in hypothesis (i), came from two irregularities that were associated with anomalous motions of visible white ovals. A methane-dark wave disappeared where white oval no.5 developed a speed slower than the wave pattern, and waves failed to appear where white oval Z was advancing faster than the wave pattern. So although the methane-dark patches tended to maintain a fixed wavelength, they could not survive when the visible disturbances adopted a conflicting motion.

In summary, our analysis shows that the waves had a fixed relationship to underlying visible tropospheric circulations. Many of the waves coincided with these circulations, and those which did not had drift rates that were more similar to the underlying visible features than to those of other waves. Therefore, individually and collectively, the waves appear to have been imposed from the tropospheric circulations according to hypothesis (i).

### *Are these waves always present?*

As noted above, these waves seemed to be a transient phenomenon in 2000/2001, just as the NEB expansion event reached completion. No such waves have been reported in previous methane images, not even those of 1994 and 1997 when the NEB was in a similar recently broadened state. The available methane image data for those years are not of such good quality as for 2000/2001,[3,35] but they could probably have shown strong wave patterns if present. Weaker or less extensive wave patterns might well have been missed; in fact there are hints of less conspicuous patterns in a HST map from 1996[46] and in some of our images from 1999/2000.[3]

### *Relationship to 'slowly-moving thermal waves' on the NEB*

For some years there has been a mystery about 'slowly-moving thermal waves' on the NEB. These have been reported in scans and images in the mid-IR, both from *Voyager* and from Earth-based IR telescopes. They have been puzzling because

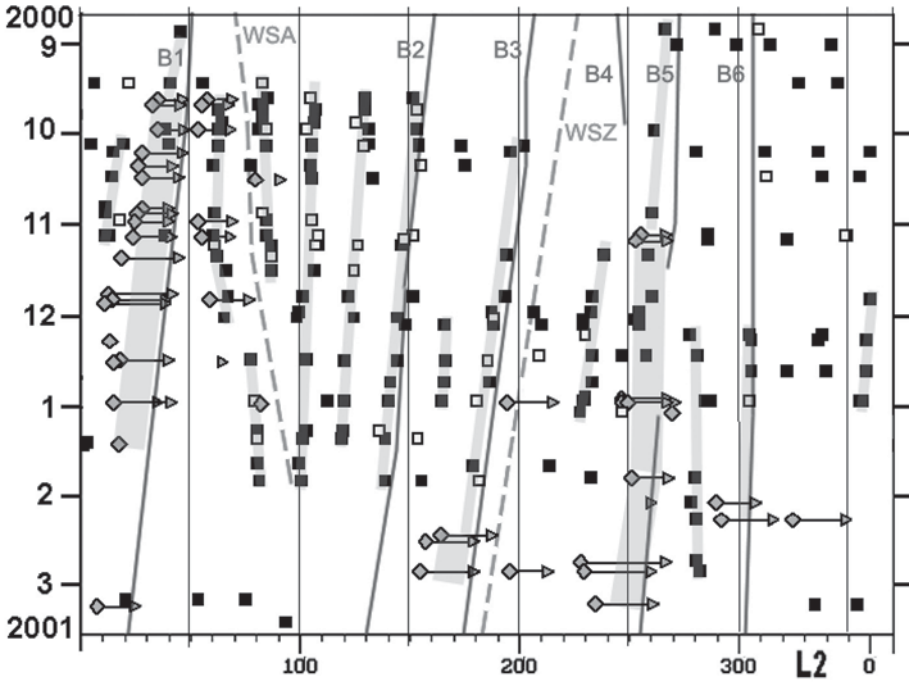


**Figure 17.** Drift chart of the NEB methane-dark waves: System II longitude versus time in months, labelled on first day of each month. Continuous lines mark the tracks of the long-lived NEB barges and white ovals (WSA, no.5; WSZ, white spot Z), from Paper I. Points mark the methane-dark patches, measured by JHR from IRTF and amateur images: diamond, p. end; triangle, f. end; square, centre; open symbols are imprecise measurements. The methane-dark waves tend to lie on the p. sides of barges and avoid white ovals.

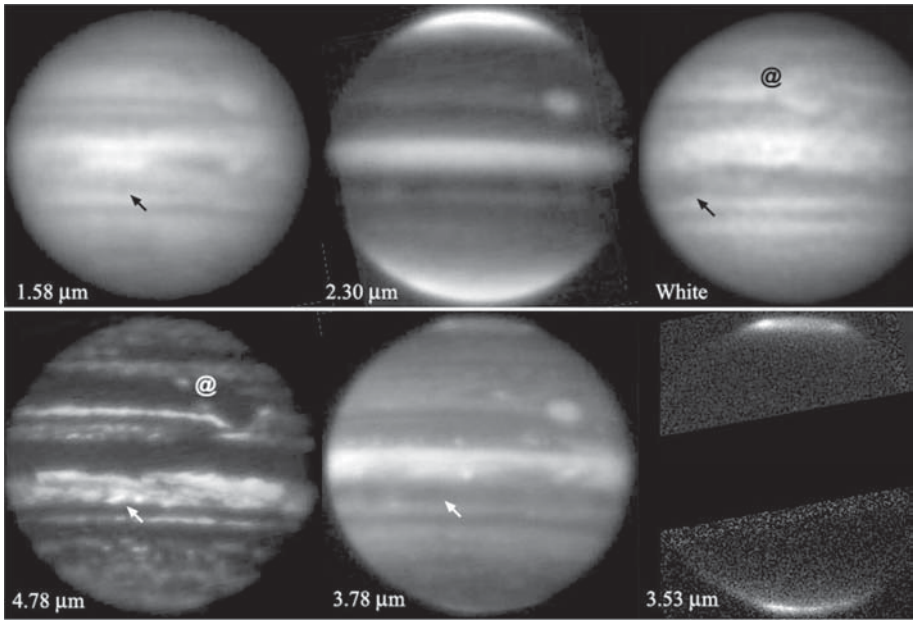


**Figure 18.** Set of IRTF images on 2001 March 6, around 04h41m UT (CM3=39, CM2=36), with a white-light image by A. Cidadão, March 7, 21h11m UT (CM2=71, CM3=67). Features include: (1) The GRS, with the brown oval no.4 (@) poised on p. edge of Red Spot Hollow; (2) The SED main complex passing the GRS (most prominent at 3.8μm); (3) Big NEBs plateaux still recorded at 1.6μm; but in 4.8μm and white light images there are just narrow strips; (4) Methane-dark NEB waves, long and irregular but the big one at barge B1 has reappeared. Arrow indicates B1 or an infrared dark spot close to it.

they appeared to be unrelated to visible features and appeared to extend over the equatorial jetstream. However, the resolution in space and/or time has been too limited to establish their true nature and motion. As we review here, the properties of these features are very similar to those of the methane-dark waves in 2000/2001; so they are probably the same phenomenon, now seen clearly for the first time.

The 'slowly-moving thermal waves' have been reported in three emission wavebands which represent three high levels in Jupiter's atmosphere:

i) ~18–20μm: pure thermal emission representing the gas temperature at the 200–300 mbar level, in the upper troposphere; i.e. at or near the top of the high-altitude haze, at about the same level as the methane-dark waves in the present report.

ii) 8–13μm: emission from the same levels and up to ~150 mbar level; but also modulated by ammonia opacity and upper tropospheric haze, as well as temperature.

iii) 7.8μm: methane emission from the 10–20 mbar level, high in the stratosphere, where brightness again represents gas temperature.

Thermal waves at the 270 mbar level were first reported by Magalhaes *et al.*[44,45] from correlation of lo-res maps derived from *Voyager* infrared spectrograms taken 4 months apart in 1979. These authors inferred that warm and cool patches all over the northern hemisphere were moving at DL2~ –13°/mth, and the equatorial region even slower. This was a surprising claim and the data did not have sufficient spatial or temporal resolution to determine the nature of these features. In fact the motion for the northern hemisphere was very close to that of the 4 prominent barges, and the 3 major warm patches were each 10–15° p. a barge. So the thermal pattern then may well have been similar to the methane-dark pattern in 2000/2001, with broad warm patches centred p. the barges and extended diffusely beyond the latitudes of the NEB.

Thermal waves at the ~150–250 mbar level were reported by Deming *et al.*,[47] on the basis of scans along the NEB and EZ with the IRTF at 8–13μm in late 1987 (although this waveband may be affected by meteorology as noted above). They revealed wave-like patterns with a wavelength of ~35° in longitude, although not fully resolved. At that time there was only one visible barge and no visible periodic pattern.

Thermal waves at the 10–20 mbar level, again mainly over the NEB, were shown in 7.8μm images from the IRTF.[48,49] They were present in all years from 1984 to 1988, and were most notable in 1985 June (periodicity of ~45° longitude) and 1988 Sep (periodicity ~33°). There were no barges in those years. No waves were observed in 1989 and 1990.

More recent IRTF observations[42,43,50] have confirmed that there are usually thermal patterns over the NEB at all three levels, that they are slow-moving relative to System II or III, that they vary in intensity and spacing, and that they sometimes change within only a few weeks. Sometimes the slow-moving patterns do extend over the EZ, but more often they essentially coincide with the NEB. (The SEB also shows thermal fluctuations but they are less periodic and less intense, except for the well-established coolness of the GRS.) The spacing of bright patches is commonly ~25–35° longitude, but sometimes there are larger patches or longer gaps. The relationship between different levels is still unclear because observations have seldom been taken simultaneously. In late 1988,[42] several major bright patches at 200–300 mbar seemed to correlate with bright patches lying 20–40° further p. at 10–20 mbar, all prograding with DL2= –11°/mth. However, in 1989 Jan,[43] the very broad wave pattern at ~150–250 mbar had little in common with the rather flat scan at 10–20 mbar.

These surveys,[42,43] especially in the 18–20μm waveband which has been repeatedly imaged from 1984 to 1993, can also be compared with the visible record from our reports in the *Journal* of the BAA. The 200–300 mbar warm patches do sometimes seem to be related to visible barges, as in 1979 (above) and in 2000/2001 (this report), but the relationship is not fixed. The warm waves have been most conspicuous at times when barges were present, even if they were only just forming or very small. Warm waves were most conspicuous from late 1988 to early 1990,[42] just after a classic NEB broadening event. In late 1988, barges were just forming with an average spacing of ~45°, whereas warm patches were periodic with a wavelength of ~30°, with no obvious relationship in the positions. In 1989 Dec, the barges were very conspicuous visually at intervals of ~30°, and there were 5 very strong warm waves, mostly centred between (not over) the barges. Both the barges and the warm waves then subsided. In 1991 Feb, a new set of prominent

barges with a regular spacing of 24° had appeared in the aftermath of a major rift, and warm waves were again present with similar spacing;[42,43] they were almost coincident with the barges or their p. edges. In early 1993, the warm waves were more prominent again, and there were also dark spots on NEBn, both preceding and during a classic NEB broadening event.

*Conclusion*

Thermal waves over the NEB are thus always present, but are most prominent when barges exist. The spacing and motion of the warm waves is similar to that of the barges. They may be centred over the barges or up to 20° p. them; but sometimes there is no clear relationship. Broadly then, these properties are the same as those of the methane-dark waves in 2000/2001, and we predict that the methane-dark waves will be shown to coincide with warm waves at the 250-mbar level. A possible model is that meanders in the NEBn jetstream, particularly where it curves around barges, give rise to thermal fluctuations which propagate upwards and prograde, so they may be centred 5–20° p. the barge at the 250-mbar level, and 20–40° further p. at the 10–20 mbar level. The variability in the spatial relationships could be because of the variable spacing of the barges; possibly this constrains the angle at which the waves can propagate upwards. However it may also reflect the meteorological state of the NEB; thus in 2000/2001, as the NEB broadening event became complete, the average length and periodicity of the methane-dark waves underwent a rapid lengthening.

In conclusion, we believe that the 2000/2001 methane images do show the thermal waves, and for the first time it has been possible to see their structure clearly and track their motion precisely.

The *Cassini* imaging team mentions that the methane-dark waves do appear to be correlated with warmer regions in yet-unpublished maps at the ~243 mbar level from the *Cassini* Composite Infrared Spectrometer.[21] Thus, when the full *Cassini* data sets are fully analysed, it may be possible to confirm the apparent relationships between methane-dark waves, high-level thermal waves, and tropospheric circulations, and perhaps to understand the complete meteorology of this striking phenomenon.

**Addresses: JHR:** 10 The Woodlands, Linton, Cambs. CB1 6UF, UK [jhr11@cam.ac.uk]
**TA:** 2-1-6 Chuou, Kanasuyama-machi, Nasa-gun, Tochigi-ken, Japan 321-06.
**GSO:** Jet Propulsion Laboratory, California Institute of Technology, 4800 Oak Grove Drive, Pasadena, California 91109, USA [go@orton.jpl.nasa.gov]

### *Note added in proof:*

The *Cassini* Composite Infrared Spectrometer maps, showing global atmospheric temperatures on dates in 2001 January, have now been published.[52] They confirm that the methane-dark waves correspond to thermal waves. In the map at a level of ~243 mbar, the most striking features are 9 warm patches at ~15°N, and 7 of them correspond to the methane-dark patches reported here. The two largest warm areas coincide with the two largest methane-dark patches (p. barges B1 and B5), and 5 other warm spots all map 3–4° p. the longitudes of other methane-dark patches. One interesting exception is a warm spot at L3= 185 which coincides with white spot Z, suggesting that a methane-dark patch either did not form here or was less visible because of the underlying bright oval. In the *Cassini* map at a stratospheric level of ~1 mbar, the only persistent features at this latitude are two large, very warm areas centred ~20° p. the two largest methane-dark patches (p. barges B1 and B5). Each of these has a warm 'tail' extending Nf., and there are indications of warm spots or waves spreading Nf. along these tails at ~1–2°/day. Thus the *Cassini* maps not only suggest a ~20° offset in longitude due to vertical propagation of the waves (agreeing with that observed by the IRTF in 1988), but also suggest complex dynamics in the stratosphere.

## References

1 Rogers J. H., Mettig H.–J., Peach D. & Foulkes M., 'Jupiter in 2000/2001, Part I: Visible wavelengths', *J. Brit. Astron. Assoc.*, **114**(4), 193–214 (2004)
2 Rogers J. H, 'Cassini and Galileo view Jupiter in stereo', *J. Brit. Astron. Assoc.,* **111**(2), 59–60 & cover (2001)
3 Rogers J. H., 'Jupiter in 1999/2000, Part II: Infrared wavelengths', *J. Brit. Astron. Assoc.* **113**(3), 136–140 (2003)
4 West R. A., Strobel D. F. & Tomasko M. G., 'Clouds, aerosols and photochemistry in the jovian atmosphere', *Icarus* **65**, 161–217 (1986)
5 Rogers J. H., *The Giant Planet Jupiter,* Cambridge University Press, 1995
6 Simon-Miller A. A., Banfield D. & Gierasch P. J., 'Color and the vertical structure in Jupiter's belts, zones, and weather systems', *Icarus* **154**, 459–474 (2001)
7 Carlson B. E., Lacis A. A. & Rossow W. B., 'Belt-zone variations in the jovian cloud structure', *J. Geophys. Res.* **99**(E7), 14623–14658 (1994)
8 Lewis J. S., 'The clouds of Jupiter and the $NH_3$–$H_2O$ and $NH_3$–$H_2S$ systems', *Icarus* **10**, 365–378 (1969)
9 Irwin P. G. J. *et al.*, 'The origin of belt/zone contrasts in the atmosphere of Jupiter and their correlation with 5-μm opacity', *Icarus* **149**, 397–415 (2001)
10 Dyudina U. A. *et al.* & the *Galileo* NIMS & SSI teams, 'Interpretation of NIMS and SSI images on the jovian cloud structure', *Icarus* **150**, 219–233 (2001)
11 Irwin P. G. J. & Dyudina U. A., 'The retrieval of cloud structure maps in the equatorial region of Jupiter using a principal component analysis of *Galileo*/NIMS data', *Icarus* **156**, 52–63 (2002)
12 Sromovsky L. A. & Fry P. M., 'Jupiter's cloud structure as constrained by *Galileo* Probe and HST observations', *Icarus* **157**, 373–400 (2002)
13 Orton G. S. *et 40 al.*, 'Earth-based observations of the *Galileo* Probe entry site', *Science* **272**, 839–840 (1996)
14 Showman A. P. & Dowling T. E., 'Nonlinear simulations of Jupiter's 5-micron hot spots', *Science* **289**, 1737–1740 (2000)
15 Rogers J. H., News note: '*Cassini* and *Galileo* reveal secrets of Jupiter's dark patches', *J. Brit. Astron. Assoc.* **111**(5), 245 (2001)
16 Chanover N. J., Kuehn D. M. & Beebe R. F., 'Vertical structure of Jupiter's atmosphere at the *Galileo* Probe entry latitude', *Icarus* **128**, 294–305 (1997)
17 Roos–Serote M. *et al.*, 'Proximate humid and dry regions in Jupiter's atmosphere indicate complex local meteorology', *Nature* **405**, 158–160 (2000)
18 Nixon C. A. *et al.*, 'Atmospheric composition and cloud structure in jovian 5-μm hotspots from analysis of *Galileo* NIMS measurements', *Icarus* **150**, 48–68 (2001)
19 Banfield D. *et al.*, 'Jupiter's cloud structure from *Galileo* imaging data', *Icarus* **135**, 230–250 (1998)
20 Gierasch P. J. *et al.*, 'Observation of moist convection in Jupiter's atmosphere',' *Nature* **403**, 628–630 (2000)
21 Porco C. C. *et al.*, '*Cassini* imaging of Jupiter's atmosphere, satellites, and rings', *Science* **299**, 1541–1547 & online supplement (2003 March 7)
22 Keay C. S. L., Low F. J. & Rieke G. H., 'Infrared maps of Jupiter', *Sky & Tel.* **44**(5), 296–297 (1972)
23 Keay C. S. L. *et al.*, 'Hi-res maps of Jupiter at 5μm', *Astrophys. J.* **183**, 1063–1073 (1973)
24 Owen T. & Terrile R. J., 'Colors on Jupiter', *J. Geophys. Res.,* **86** (A10), 8797–8814 (1981)
25 *Cassini* mission website: **http://saturn.jpl.nasa.gov/**
26 *Cassini* imaging science team web site: **http://ciclops.lpl.arizona.edu/**
27 Moreno F., 'The structure of the stratospheric aerosol layer in the equatorial and south polar regions of Jupiter', *Icarus* **124**, 632–644 (1996)

28 Vincent M. B. *et al.*, 'Mapping Jupiter's latitudinal bands and Great Red Spot using HST/WFPC2 far-ultraviolet imaging', *Icarus* **143**, 189–204 (2000)
29 Vincent M. B. *et al.*, 'Jupiter's polar regions in the ultraviolet as imaged by HST/WFPC2: Auroral-aligned features and zonal motions', *Icarus* **143**, 205–222 (2000)
30 NASA Planetary Data System, http://pds-imaging.jpl.nasa.gov/Atlas
31 International Outer Planets Watch website: http://atmos.nmsu.edu/ijw/current_images.htm
32 Rogers J. H., Interim report: 'Jupiter in 1997', *J. Brit. Astron. Assoc.,* **107**(6), 333–335 (1997)
33 Sanchez–Lavega *et al.*, 'Dynamics and interaction between a large-scale vortex and the Great Red Spot on Jupiter', *Icarus* **136**, 14–26 (1998)
34 Rogers J. H., 'Jupiter in 1997', *J. Brit. Astron. Assoc.* **111**(4), 186–198 (2001)
35 Rogers J. H., Foulkes M. & Miyazaki I., 'Appendix: Methane band images of Jupiter, 1995–1997', *J. Brit. Astron. Assoc.* **111**(4), 197–198 (2001)
36 Rogers J. H., Mettig H.–J., Peach D. & Foulkes M., 'Jupiter in 1999/2000, Part I: Visible wavelengths', *J. Brit. Astron. Assoc.* **113**(1), 10–31 (2003)
37 Garcia–Melendo E. *et al.*, 'Long-lived vortices and profile changes in the 23.7°N high-speed jovian jet', *Icarus* **146**, 514–524 (2000)
38 Orton G. S. *et al.*, 'A cold hole at the pole of Jupiter', Abstract 13.01 for DPS meeting (2002), & image PIA03864 on PDS website (*op.cit.*, ref.30)
39 Doyle L. R. & Borucki W. J., 'Jupiter lightning locations', in *Time-Variable Phenomena in the Jovian System,* NASA SP-494 (eds. Belton M. J. S. *et al.*), 384–389, NASA, 1989
40 Borucki W. J. & Magalhaes J. A., 'Analysis of *Voyager 2* images of jovian lightning', *Icarus* **96**, 1–14 (1992)
41 Little B. *et al.* & the *Galileo* SSI team, '*Galileo* images of lightning on Jupiter', *Icarus* **142**, 306–323 (1999)
42 Orton G. S. *et al.*, 'Spatial organization and time dependence of Jupiter's tropospheric temperatures, 1980–1993', *Science* **265**, 625–631(1994)
43 Deming D. *et al.*, 'Observations and analysis of longitudinal thermal waves on Jupiter', *Icarus* **126**, 301–312 (1997)
44 Magalhaes J. A. *et al.*, 'Slowly moving thermal features on Jupiter', *Nature* **337**, 444–447 (1989); also see review by Rogers J. H., *J. Brit. Astron. Assoc*. **99**(3), 117 (1989)
45 Magalhaes J. A. *et al.*, 'Zonal motion and structure in Jupiter's upper troposphere from *Voyager* infrared and imaging observations', *Icarus* **88**, 39–72 (1990)
46 Deming D *et al.*, 'A search for p-mode oscillations of Jupiter: Serendipitous observations of nonacoustic thermal wave structure', *Astrophys. J.* **343**, 456–467 (1989)
47 Simon–Miller A. A., Banfield D. & Gierasch P. J., 'An HST study of jovian chromophores', *Icarus* **149**, 94–106 (2001)
48 Beebe R. F., Orton G. S. & West R. A., 'Time-variable nature of the jovian cloud properties and thermal structure: an observational perspective', in: *Time-Variable Phenomena in the Jovian System, op.cit.* (ref.39), 245–288
49 Orton G. S. et al., 'Thermal maps of Jupiter: Spatial organization and time dependence of stratospheric temperatures, 1980–1990', *Science* **252**, 537–542 (1991)
50 Fisher B. M., Ph.D thesis (1994), cited in ref.43.
51 Vasavada A. *et al.*, '*Galileo* imaging of Jupiter's atmosphere', *Icarus* **135**, 265–275 (1998)
52 Flasar F. M. *et al.*, *Nature* **427**, 132–135 (2004)


*Received 2003 September 08; accepted 2003 October 29*